

NEUTRINO DETECTOR DEVELOPMENTS*

James K. Walker

July 1978

* Invited talk at the International Conference on Neutrino Physics and Neutrino Astrophysics, Purdue University, April 28-May 2, 1978

NEUTRINO DETECTOR DEVELOPMENTS

James K. Walker

Fermilab

Batavia, Illinois 60510

ABSTRACT

A review is given of the new neutrino detectors which are being constructed at several laboratories. The detection characteristics of each detector are briefly described and summarized. New ideas and proposals for additional neutrino detectors are also discussed in some detail.

I. INTRODUCTION

In the last year, there has been great progress in bringing into operation new and more powerful electronic neutrino detectors. At all of the major Laboratories there is an intense effort to develop neutrino detectors which can address fundamental physics issues involving neutrinos. I will not review the traditional calorimetric detectors employed by the collaborations of (a) California Institute of Technology, Fermilab (b) Harvard, Pennsylvania, Wisconsin, Fermilab, and (c) CERN, Dortmund, Heidelberg, Saclay. I will begin by describing the properties of the new detectors which are being constructed at the various Laboratories. Then I will outline several new imaginative ideas for the next generation of detectors.

The description of the new detectors will be grouped according to physics topic. These are:

1. Semi-Leptonic Inclusive Scattering

- A. CHARM collaboration at CERN
- B. FIMM collaboration at Fermilab

2. Elastic Neutrino Electron Scattering

- A. Virginia, Maryland, Oxford collaboration at Fermilab
- B. FIMM collaboration at Fermilab
- C. CHARM collaboration at CERN
- D. Brookhaven, Pennsylvania collaboration at B.N.L.
- E. Irvine, Los Alamos collaboration at Los Alamos

3. Search for short-lived particle production by neutrinos.

Finally, in the realm of new ideas and techniques which have been proposed, we shall outline:

4. The Liquid Argon Time Projection Chamber
5. The Liquid Argon Iron Plate Calorimeter
6. The Liquid Argon Bubble Chamber with Electronic Readout
7. The Water Cerenkov Neutrino Detector
8. A Search Method for Massive Neutral Leptons.

II. NEW DETECTORS

1. Semi-Leptonic Inclusive Scattering

The kinematics of inclusive neutrino scattering are illustrated in Figure 1.

The neutrino cross section can be expressed as a function of two variables x and y . A determination of the values of the scaling variables, x and y , in neutral current inclusive scattering can be made if θ_H and E_H are measured. θ_H is defined as the angle of energy flow of the hadronic system.

$$\theta_H = \frac{\sum_i E_i \theta_i}{\sum_i E_i}$$

where θ_i and E_i are the angle and energy of the i^{th} hadron produced in the interaction and $E_H = \sum E_i$.

There are two new detectors being constructed at CERN and Fermilab which, for the first time, will permit a measurement of θ_H and E_H , or equivalently, x and y , for neutral current inclusive scattering.

A. The experiment (WA-18) at CERN is by the CHARM (CERN, Hamburg, Aachen, Rome, Moscow) collaboration. This detector has been constructed and is set up behind the WA-1 neutrino apparatus. A series of 8 cm thick marble plates are interspersed with detector elements as shown in Figure 2. These elements are used to perform the following measurements:

- (i) the lateral position of the interaction vertex to determine both the incident neutrino energy in the narrow-band beam and the origin of the vector of the energy flow;
- (ii) the magnitude and direction of the hadron energy flow;
- (iii) the direction of charged tracks inside the predicted

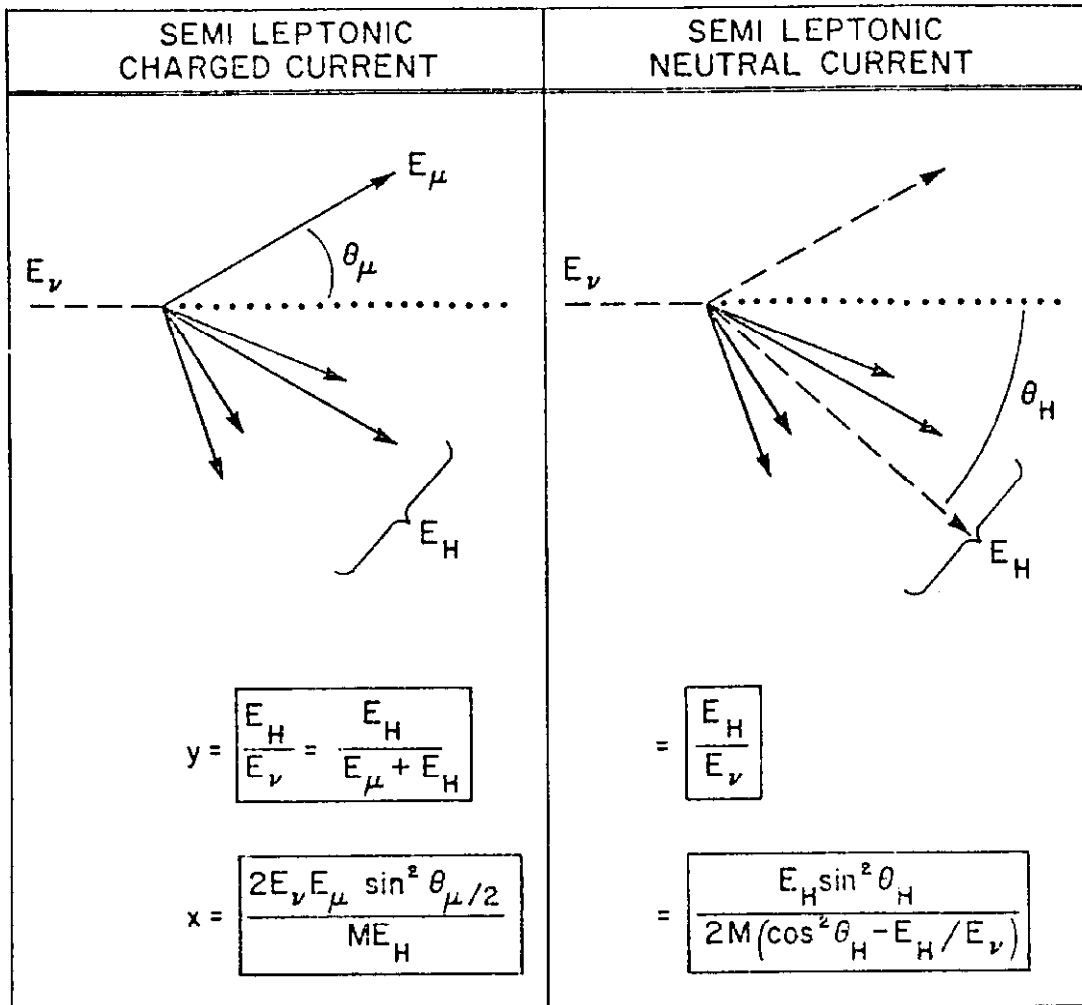


Figure 1.

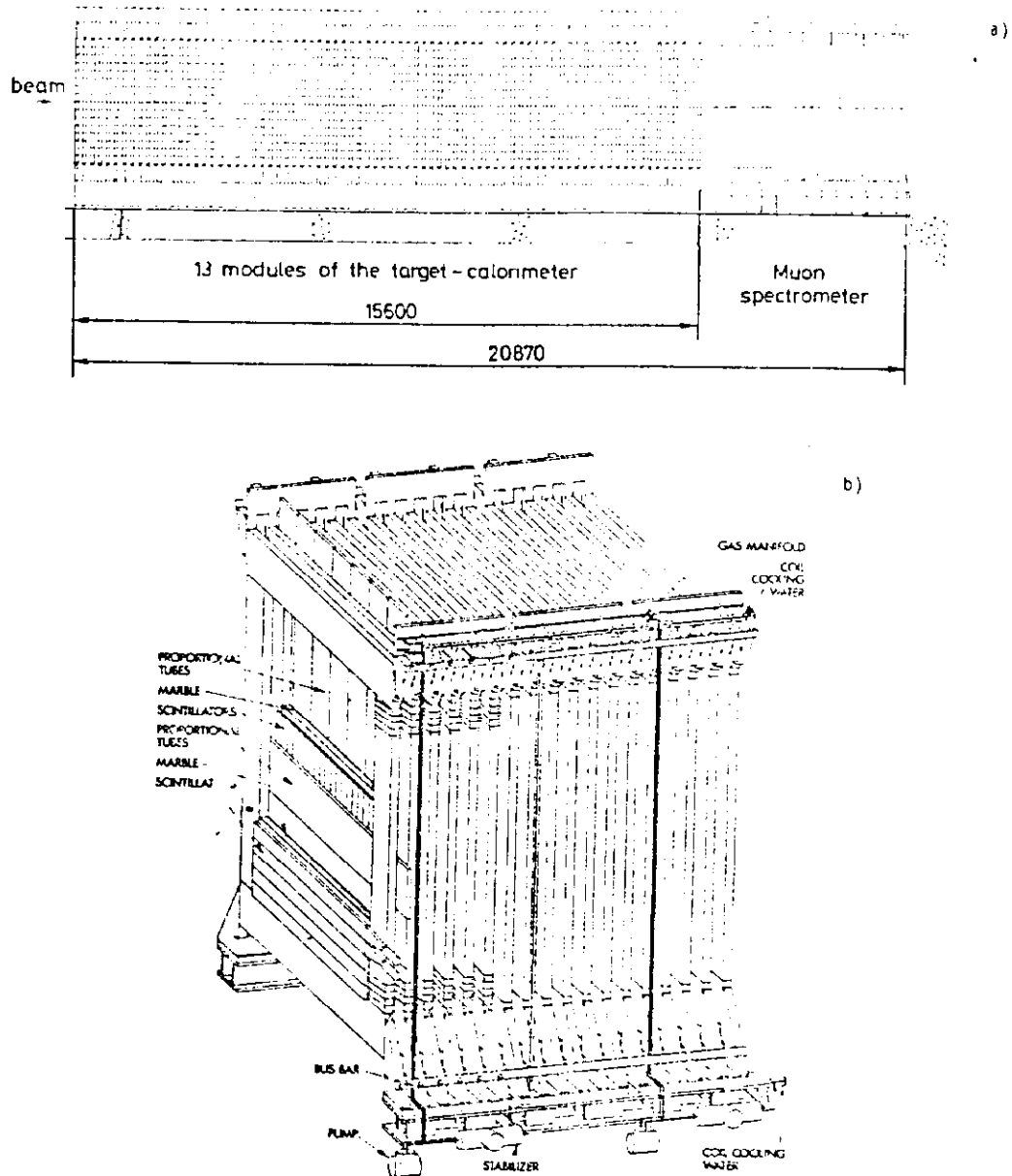


Figure 2

Figure 2. - a) General layout of the CHARM detector, b) Details of one module of the calorimeter.

cone of the outgoing lepton for muon identification.

Events with muons from π or K decay are ambiguous; they can be properly assigned by measuring the muon momentum and checking the total visible energy against the a priori known neutrino energy. To perform this momentum measurement, a magnetized iron shell surrounds the entire hadron calorimeter.

The detector elements employed between the marble sheets are scintillation counters for the measurements of the magnitude and the direction of the hadron energy flow and proportional counters for the determination of the shower apex and following charged particle tracks. Scintillation counter hodoscopes are alternately in the x- and y- directions, with each hodoscope between the marble slabs as shown in Figure 2. Each counter is 15 cm wide, transverse to the beam axis. The proportional counters are arranged in the y- and x- directions relative to the scintillation counter hodoscopes. Each tube is 3 cm wide. The plate thickness, material and widths of the detector elements were chosen to optimize the performance in measuring the energy and direction of the hadron shower. This direction is determined by the line joining the shower vertex and the centers of gravity of the shower in each detector plane. This is obtained from the mean value of the detector cell coordinates, weighted with the pulse height in each cell, e.g.,

$$\langle \theta \rangle = \frac{\sum_i Q_i \theta_i}{\sum_i Q_i}$$

The results of a Monte Carlo simulation of the detector response are shown in Figures 3a and 3b. We may note that for this purpose aluminum and marble are quite similar. This demonstrates that the intrinsic resolution due to shower fluctuations is about + 7 mrad for a 100 GeV hadronic shower. For the configuration of this detector, an angle resolution of + 10 mrad is expected at 100 GeV. Data from a test beam at 22 GeV are shown in Figure 4 and give $\sigma(\theta_H) = 38$ mrad. It is hoped to improve this

resolution using proportional counter information in addition to the scintillation counters for the determination of the centers of gravity of the developing shower. In this case, the experimenters anticipate that the projected angle resolution, $\sigma(\theta_H)$, for this detector can be parameterized as:

$$\sigma(\theta_H) = 4 + \frac{600}{E_H} \text{ mr (} E_H \text{ in GeV).}$$

The anticipated energy resolution is:

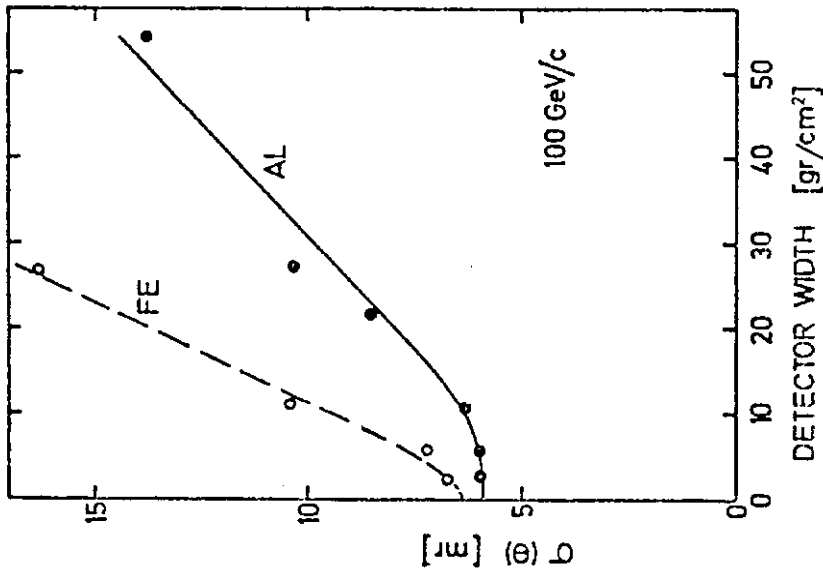


Figure 3a

Resolution $\sigma(\theta_H)$ on the hadron shower direction (assuming the apex position is known) as a function of the width of the detector elements, $\rho \cdot \Delta r$, for Al and Fe plates, where ρ is the average density ($E_H = 100$ GeV).

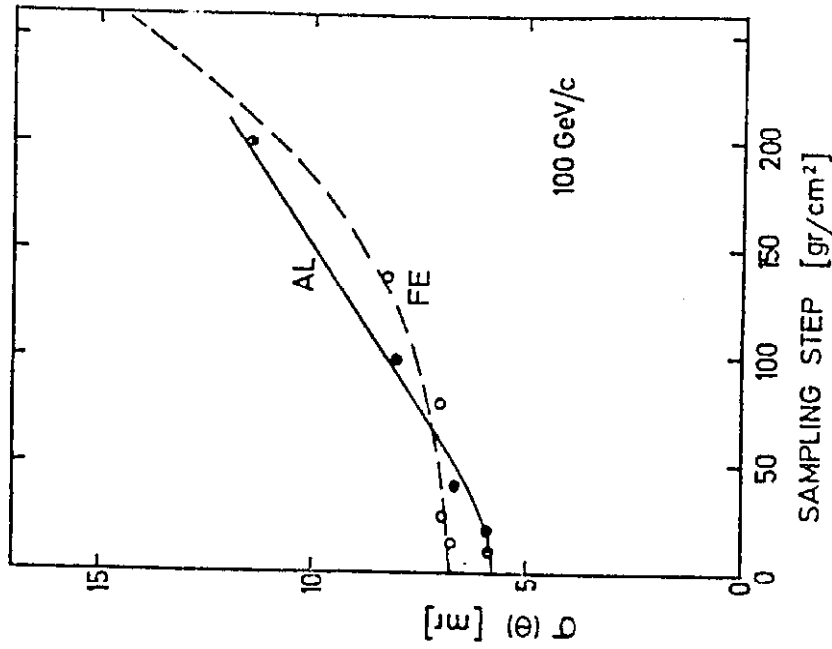


Figure 3b

Resolution $\sigma(\theta_H)$ on the hadron shower direction as a function of sampling step, $\rho \cdot \Delta t$ ($E_H = 100$ GeV).

Figures 3a & 3b.

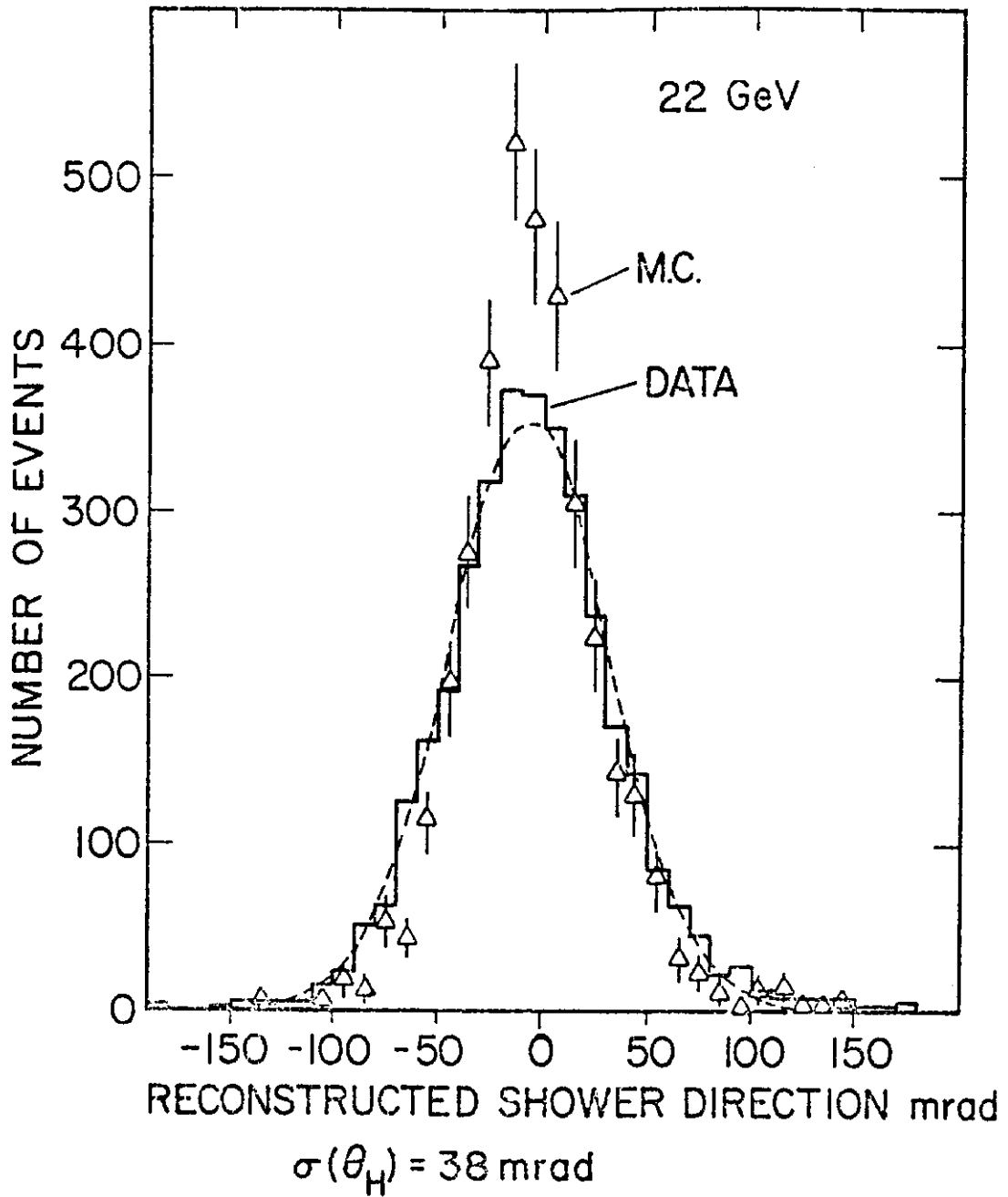


Figure 4. - CHARM test calorimeter data for 22 GeV hadrons. The Monte Carlo simulation is in approximate agreement with the data. The measured projected angle resolution, $\sigma(\theta_H)$, of reconstruction of the hadron shower direction is 38mrad at 22 GeV.

$$\frac{\sigma(E_H)}{E_H} = \frac{55\%}{\sqrt{E_H \text{ (GeV)}}$$

At the downstream end of the calorimeter, there is a series of magnetized iron toroids. These are used to determine the momenta of muons to $(\Delta p/p) = \pm 15\%$. A sample of charged current events will be recorded for calibration purposes.

The resolution in the scaling variable x has been calculated by a Monte Carlo method. The calculation takes into account

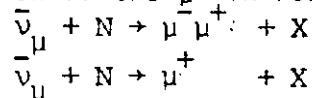
- (i) The error in neutrino energy corresponding to a parent beam momentum bite of $\pm 2.7\%$;
- (ii) Hadron energy measurement error;
- (iii) Angle of hadron energy flow error.

The resulting resolution for x is shown for the case of 240 GeV neutrinos.

$y \setminus x$	0.1	0.3	0.5	0.7	0.9
0.1/0.2	0.06	0.11	0.16	0.19	0.23
0.2/0.4	0.05	0.10	0.15	0.18	0.21
0.4/0.6	0.07	0.13	0.15	0.19	0.23
0.6/0.8	0.10	0.16	0.22	0.26	0.30

This resolution is adequate to study in detail the structure functions in semi-leptonic neutral current interactions.

An interesting additional attribute of this detector is its ability to measure the polarization of positive muons. In collaboration with WA-1 experimenters they intend studying the polarization of the μ^+ in reactions:



The events of interest will occur in the WA-1 detector and the μ^+ will be ranged out in the CHARM detector. A field of about 40 gauss on the whole detector will be produced by appropriate energizing of the coils for the iron shell surrounding the calorimeter. Approximately 50,000 stopped μ^+ from the former

of the two reactions is expected for one week of wide band antineutrino running. An accuracy of polarization of $\pm 5\%$ is expected under these conditions.

A summary of the properties of this detector are:

Total Calorimeter Mass: 200 Tons
Angle Resolution: $\sigma(\theta_H) = (4 + 600/E_H)$ mrad
Hadron Energy Resolution: $\frac{\sigma(E_H)}{E_H} = 55\%/E_H$

B. At Fermilab a new collaboration, FIMM, (Fermilab, Northern Ill. Univ. at DeKalb, MIT, MSU) E-594, is constructing a flash chamber detector to study neutral current inclusive scattering. The 400 ton detector will be located in front of the existing 24-ft. diameter iron toroids previously used by the HPWF collaboration. A module of the detector is shown in Figure 5.

Flash chambers²₃ are alternated with 3/8" thick asbestos sheets ($\rho = 1.85 \text{ g/cm}^3$) for the full length of the detector. The detector is triggered by proportional chamber planes located at one foot intervals throughout the detector. The flash chambers are constructed from extruded polypropylene plastic at a cost of \$1.50/sq. meter. The individual cells of plastic are 5mm x 5mm cross section and are filled with the standard spark chamber gas of 90% Ne + 10% H₂. Gas manifolds are thermo-vacuum formed from UVAC plastic. The polypropylene planes are covered with aluminum foil to form the electrodes. When an event of interest is detected by the proportional counters, a high voltage pulse of 5 KV is applied across the flash chambers thereby causing a glow discharge in the tubes where the particles traversed the chambers. The cement sheets are similar to aluminum in regard to radiation length and collision length but are considerably less expensive.

Hadron showers were measured in a test beam with a prototype flash chamber calorimeter constructed similar to that described above. The hadron energy range was 5 to 300 GeV. Some observed hadron cascades are shown in Figure 6. The hadronic cascades were used to simulate the hadrons produced in neutrino interactions. The hadron energy flow direction of the particles emerging from the interaction point is determined by a least squares fit to the primary vertex position and the center of gravity coordinates of the hadron cascade in each flash chamber plane. Figure 7 shows measurements of 40 GeV hadron cascade development in the detector. Data is shown only every ninth plane for the sake of clarity. The measured energy flow projected angle resolution $\sigma(\theta_H)$ is shown plotted versus $1/E_H$ in Figure 8. The data can be described roughly by the expression:

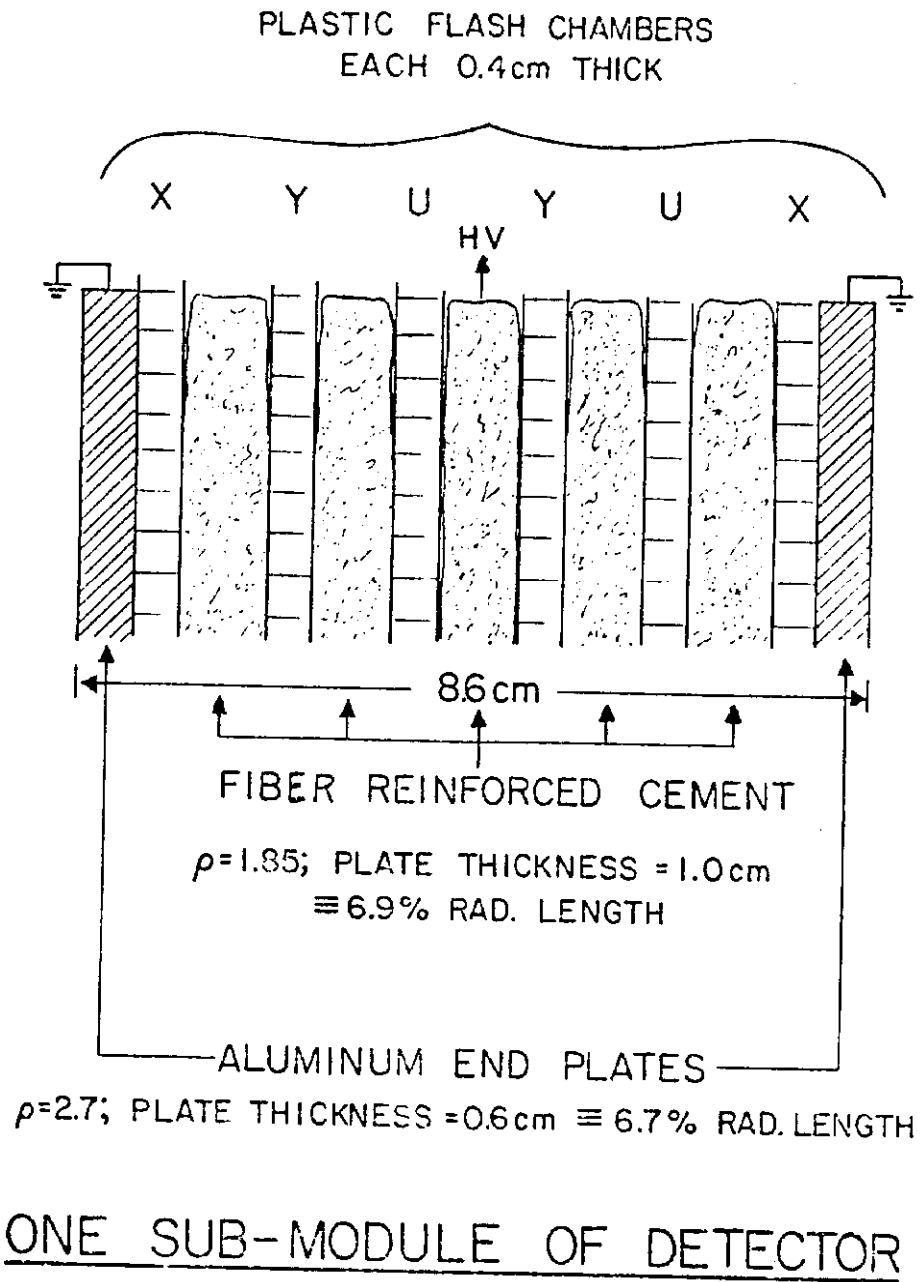


Figure 5

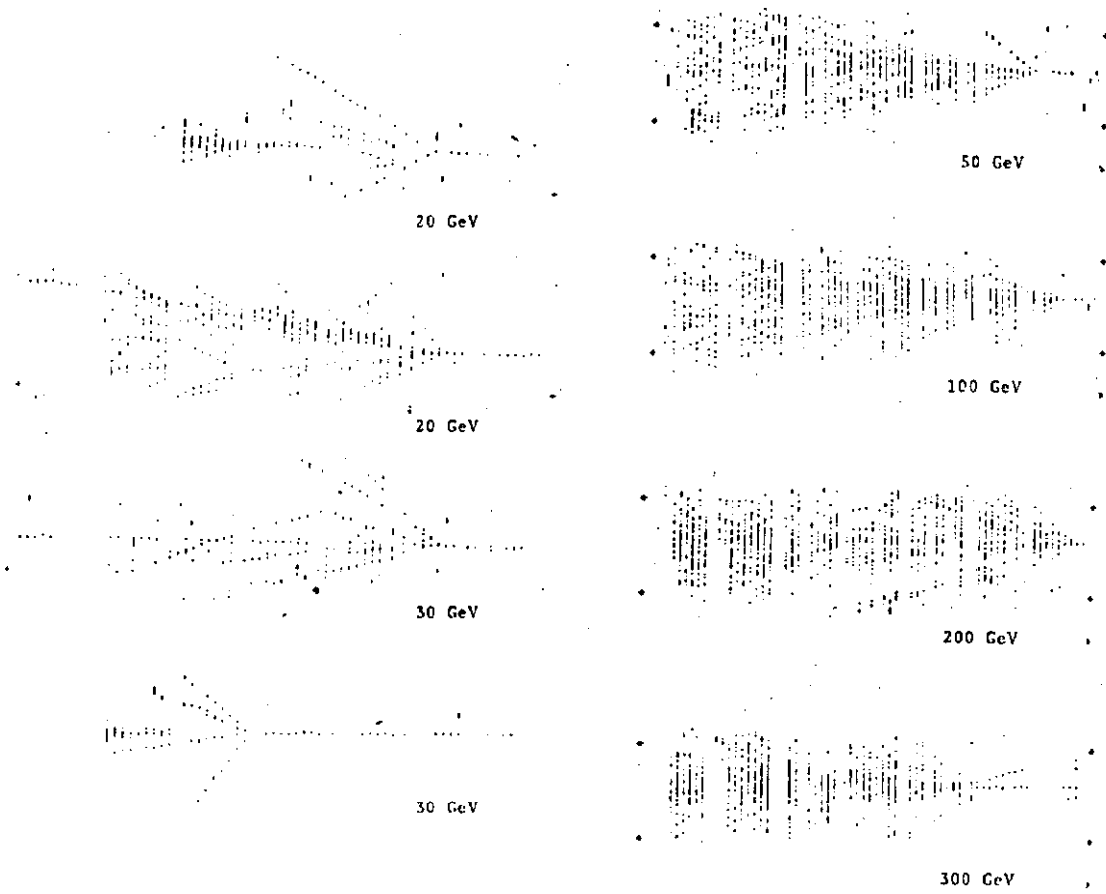


Figure 6. - FIMM test calorimeter photographs of hadron cascades. The energy of the incident hadron is indicated in the figure.

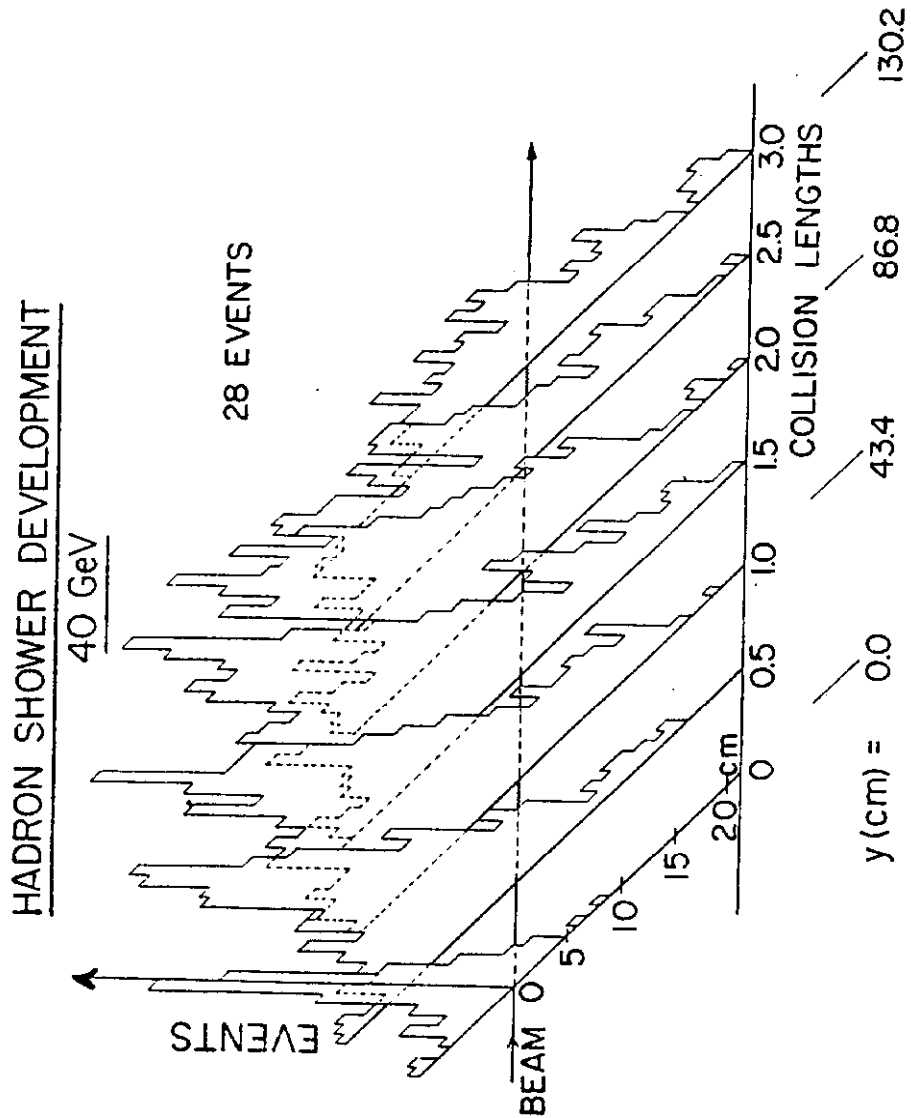


Figure 7. - Transverse and longitudinal structure of 40 GeV hadronic cascades in the FIMM test calorimeter. Only every ninth plane is shown for clarity.

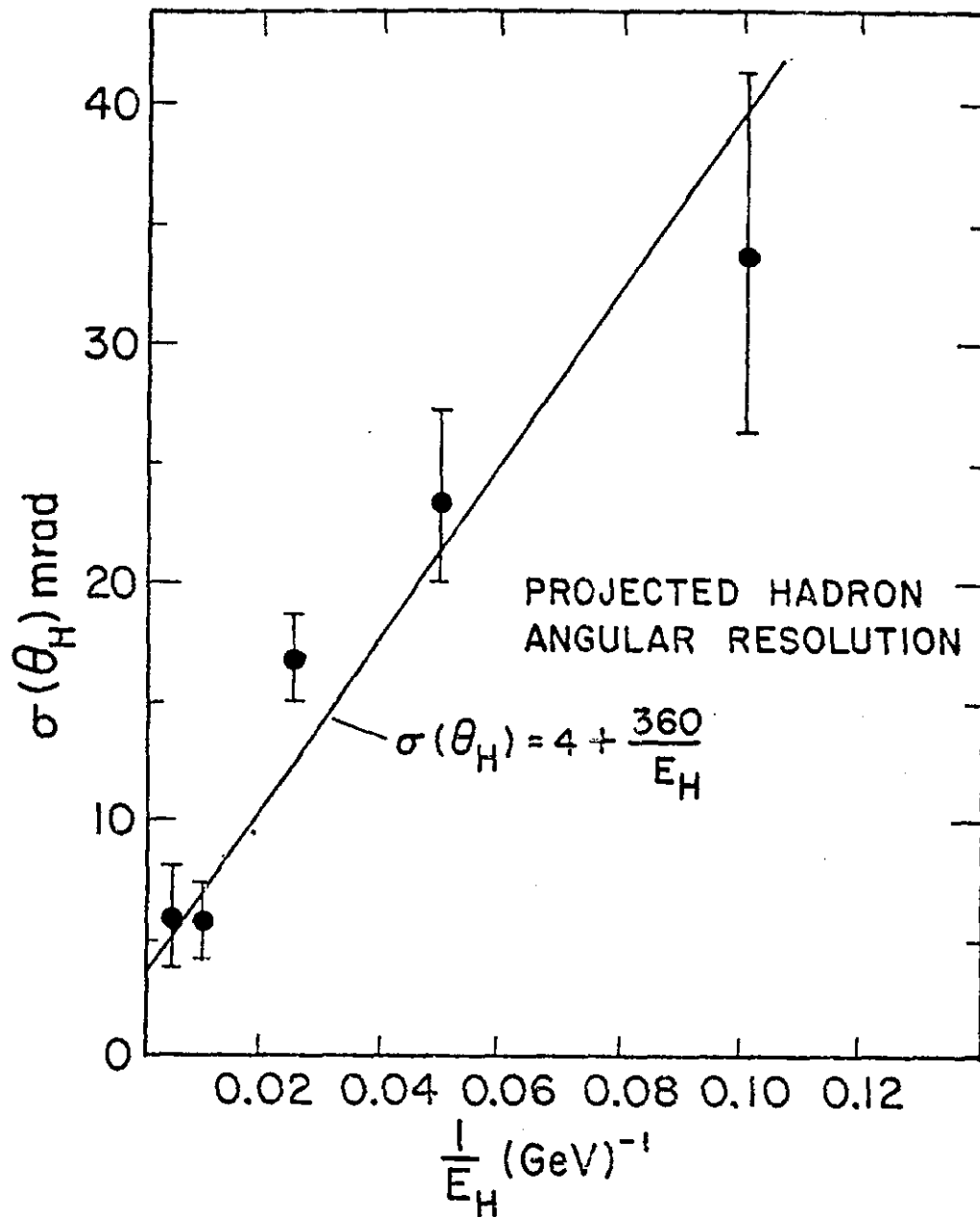


Figure 8. - The projected angle resolution, $\sigma(\theta_H)$, for hadronic cascade development is shown plotted against the inverse of the hadron energy. The data was obtained with the FIMM test calorimeter.

$$\sigma(\theta_H) = 4 + 360/E_H \text{ (GeV) mrad}$$

This is in good agreement with the previously described Monte Carlo estimates based on sampling the hadron cascade with this frequency both transversely and longitudinally. The calculations suggest that this measuring accuracy is limited by fluctuations in the development of the cascade and further subdivision of the detector will not improve angle resolution.

The total number, N , of flash chamber cells which fire provide a measurement of the total hadronic energy, E_H , see Figure 9a. Fluctuations of that number, $\sigma(N)$, lead to an error, $\sigma(E_H)$ in the energy estimate. As the size of the prototype calorimeter was adequate to contain only about 50% of the total energy, a correction to N and $\sigma(N)$ was made on the basis of previous measurements.³ The resulting energy resolution, $\sigma(E_H)/E_H$, is plotted versus E_H in Figure 9b. The reliability of these corrections are uncertain but the energy resolution will be measured with a hadron beam into the full size detector. The resolution is roughly constant over the entire energy interval of 10 to 200 GeV. This is because the natural $1/\sqrt{E_H}$ improvement with energy is balanced by the essential non-linearity of the energy response of the detector - due to finite size cells. However, it is interesting that the energy resolution appears to be so good. There are several possible reasons for this good resolution. The digital nature of the flash chamber removes the large fluctuations due to nuclear fragments and delta rays which occur in linear detectors. In addition, the flash chambers sample the hadron shower very finely (every 3.5% of a collision length). Finally, due to the reasonably low average atomic number, the radiation length and collision length of cement are not dissimilar (about 18 and 46 cm respectively). This minimizes fluctuations due to cascades which are largely electromagnetic, or are largely hadronic.

An electronic readout system has been developed to record the data from the flash chambers. Figure 10 shows a schematic of the system. Current from the plasma flows to ground via the holes in the plastic. A few amperes is adequate to produce a signal in a magnetostrictive line used in the conventional manner. The pulses at the output of the amplifier are separated in time, even in the case of adjacent firing cells.

The advantages of the use of plastic flash chambers are low cost, excellent multi-track capability due to the very low currents involved with each track and a simple inexpensive readout system.

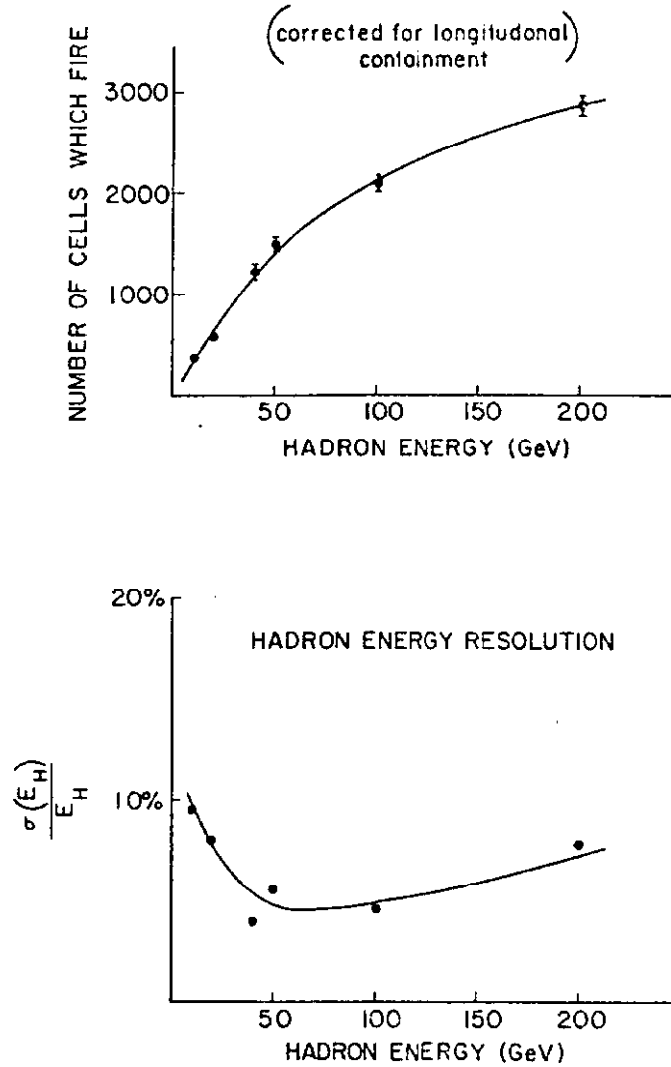


Figure 9. - a) The number of firing cells, corrected for longitudinal containment is plotted versus hadron energy. b) The energy resolution $\sigma(E_H)/E_H$ of the FIMM test calorimeter is plotted vs. the hadron energy. These data are tentative due to the large corrections which were applied to compensate for the approximately 50% energy containment as described in the text.

CHAMBER CONSTRUCTION FOR MAGNETOSTRICTIVE READOUT

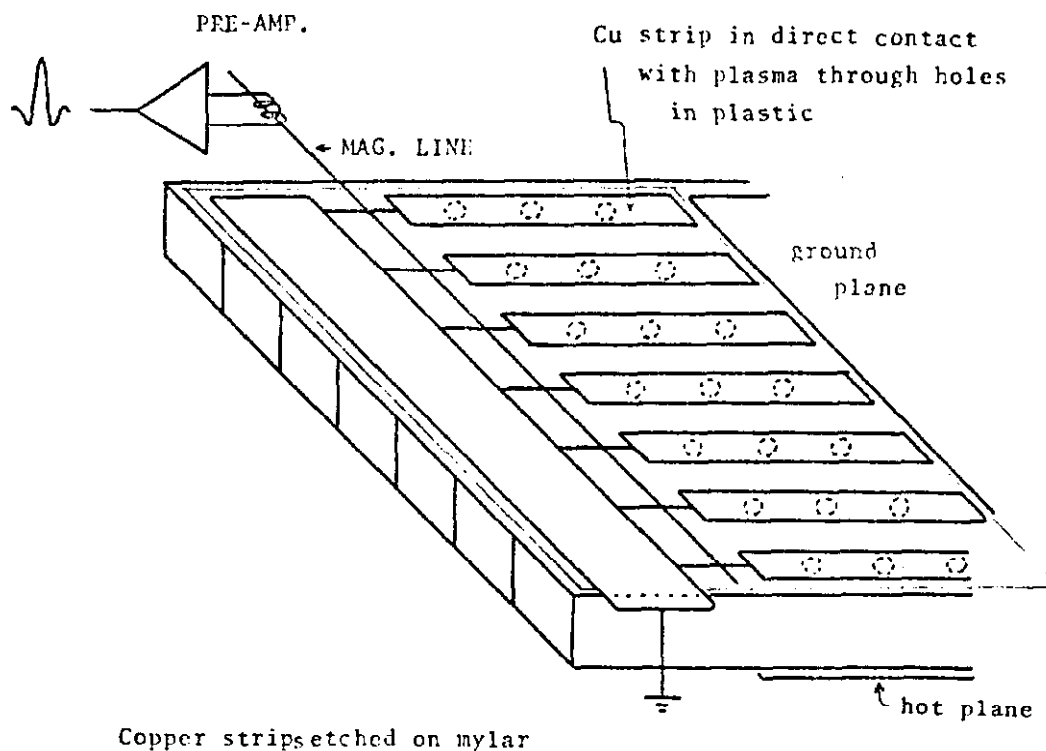


Figure 10. - Electronic readout system for the flash chambers of the FIMM detector. Several amperes flow to ground when a cell fires. This is adequate to produce a magnetostrictive signal which is detected in the conventional manner.

A summary of the properties of this detector are:

Total Calorimeter Mass:	400 Tons
Angle Resolution:	$\sigma(\theta_H) = (4 + 360/E_H)$ mrad.
Hadron Energy Resolution:	$\sigma(E_H)/E_H = 6\%$ for $E_H > 10$ GeV.

2. Elastic Neutrino Electron Scattering

There are five detectors in various stages of preparation which will attempt the difficult measurement of neutrino electron elastic scattering. All of the detectors rely on excellent angle resolution for the very forward scattered recoil electron.

A. A Virginia, Maryland, Oxford collaboration (E-253) working at Fermilab has constructed a 20 ton detector whose sole aim is the study of the reaction:



The apparatus is complete and is shown in Figure 11. It is ready to begin data taking runs. Figure 12 shows a schematic of the detector. A nine centimeter thick plate of aluminum is followed by a scintillation counter and multiwire proportional chamber. This sequence is repeated 43 times. The transverse dimensions of the detector are 1m x 1m. Figure 13 shows the track location in the x and y planes of a single muon traversing the detector. The third plot in the figure shows the pulse height distribution in each plane of the scintillation counters. Figure 14 shows a candidate for a neutrino electron elastic scattering event. A zero angle event is observed near the front of the detector with the characteristics of an electromagnetic rather than hadronic cascade. The angle resolution of the detector for 4 GeV electrons has been measured to be 4 milliradians. In addition, a pion rejection of 300:1 has been measured. This hadron rejection was obtained by studying the pulse height distribution in the scintillation counters using a 10 GeV test beam composed of pions and electrons. The pulse height spectra are shown in Figure 15. Cuts were applied in each counter to achieve an electron efficiency of 90% and a pion rejection factor of 300:1. Additional pion rejection should be obtained by studying the transverse structure of the cascade.

The detector is located in the middle of the muon shield of the neutrino beam. The backgrounds for 400 GeV running are high but it is hoped that with the addition of magnetized iron toroids upstream at the front of the shield, the stray muon flux will



Figure 11 . - The Virginia, Maryland, Oxford detector at Fermilab for neutrino electron elastic scattering.

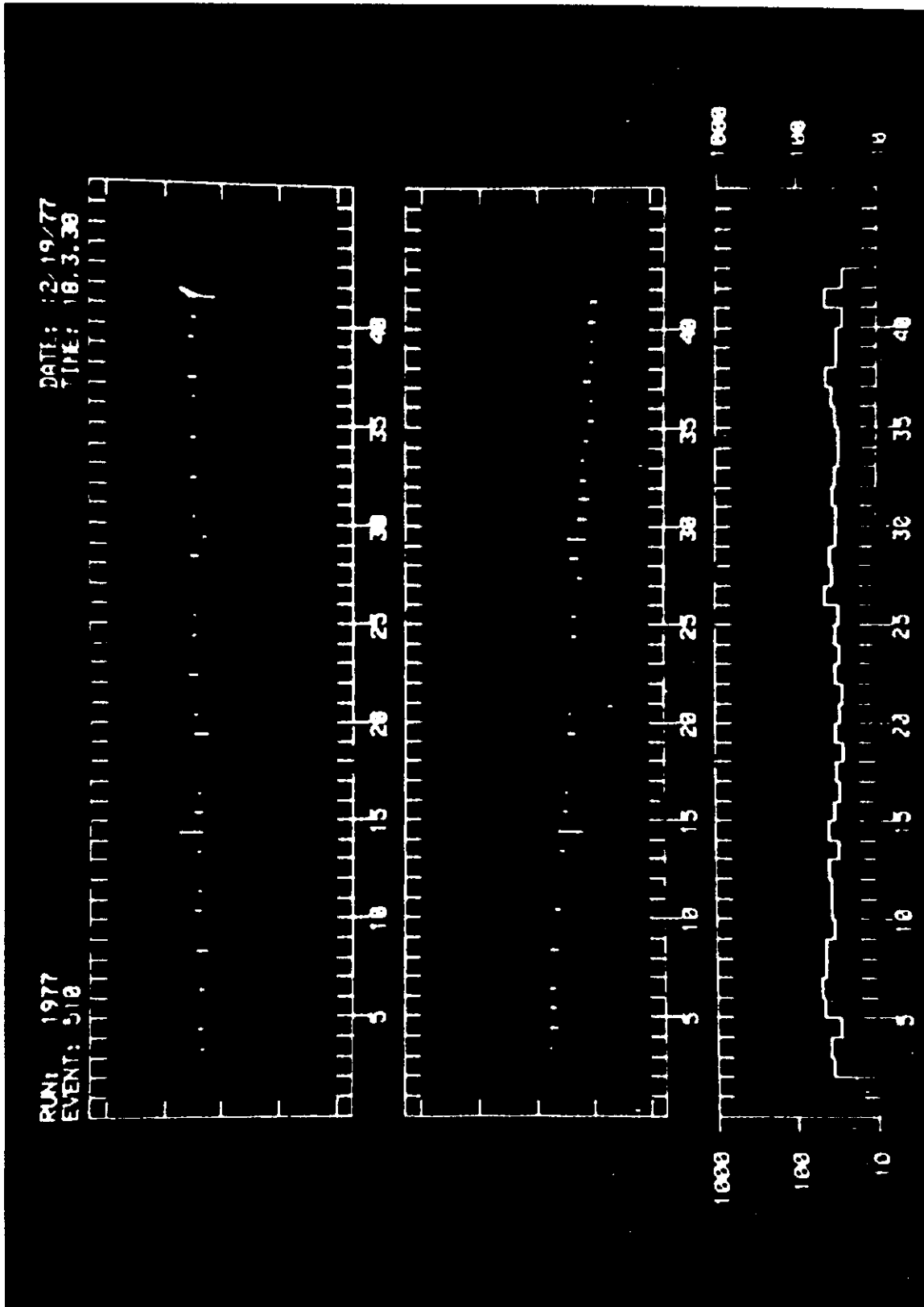


Figure 13. - A single muon event traversing the Virginia, Maryland, Oxford detector. The upper two plots show the trajectory in two orthogonal views. The lower plot shows the pulse height observed in each of the 43 scintillation counters.

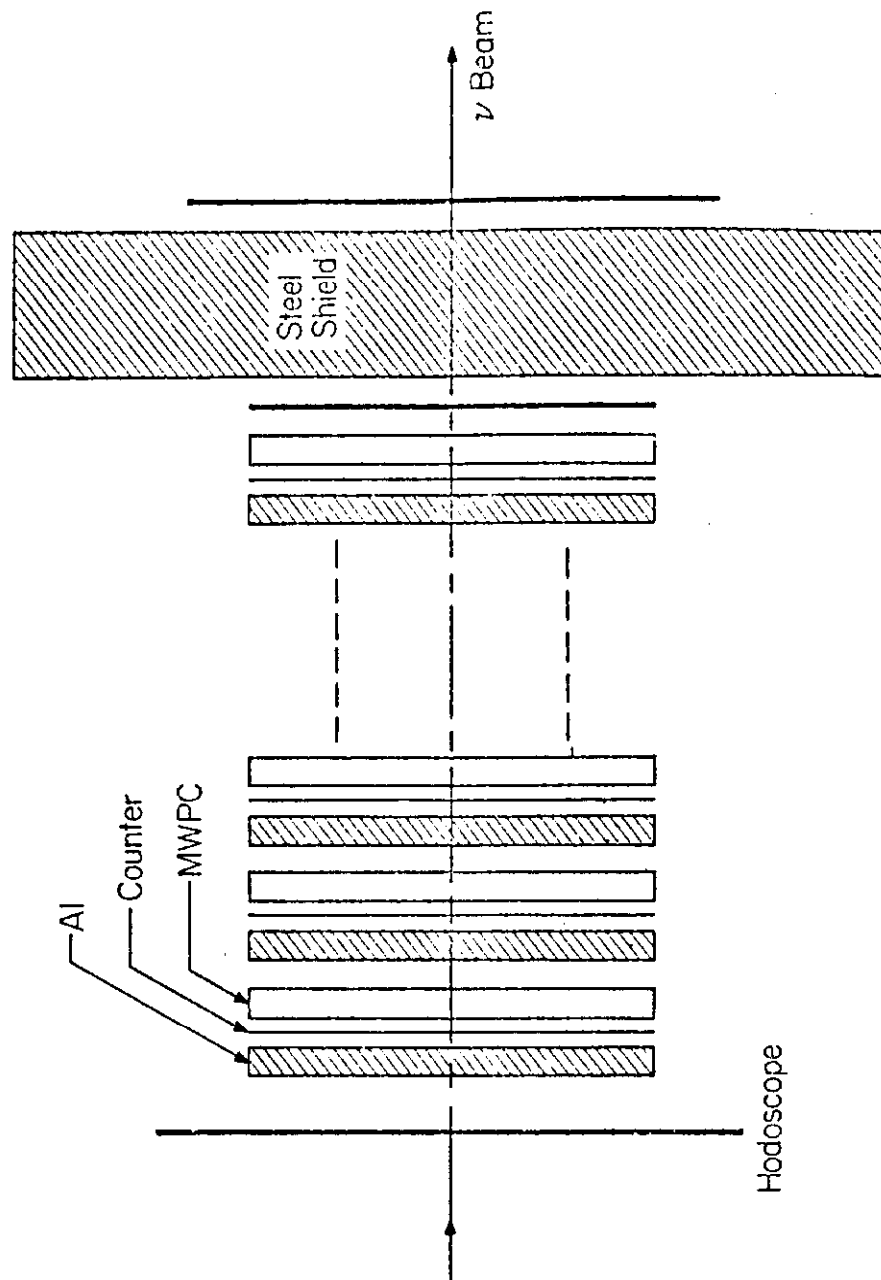


Figure 12. - Schematic of the Virginia, Maryland, Oxford detector.

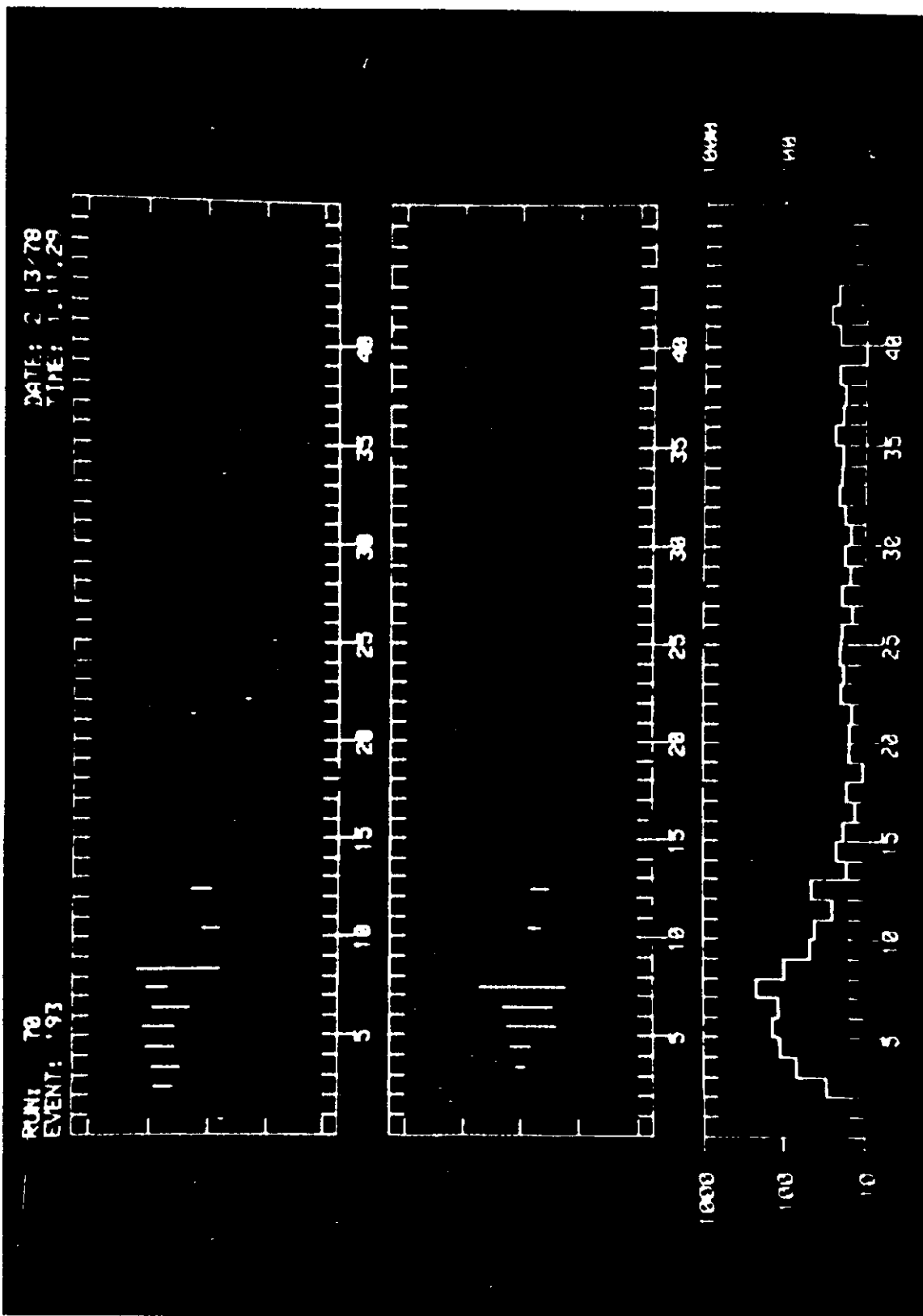


Figure 14. - A candidate for neutrino electron elastic scattering in the Virginia, Maryland, Oxford detector.

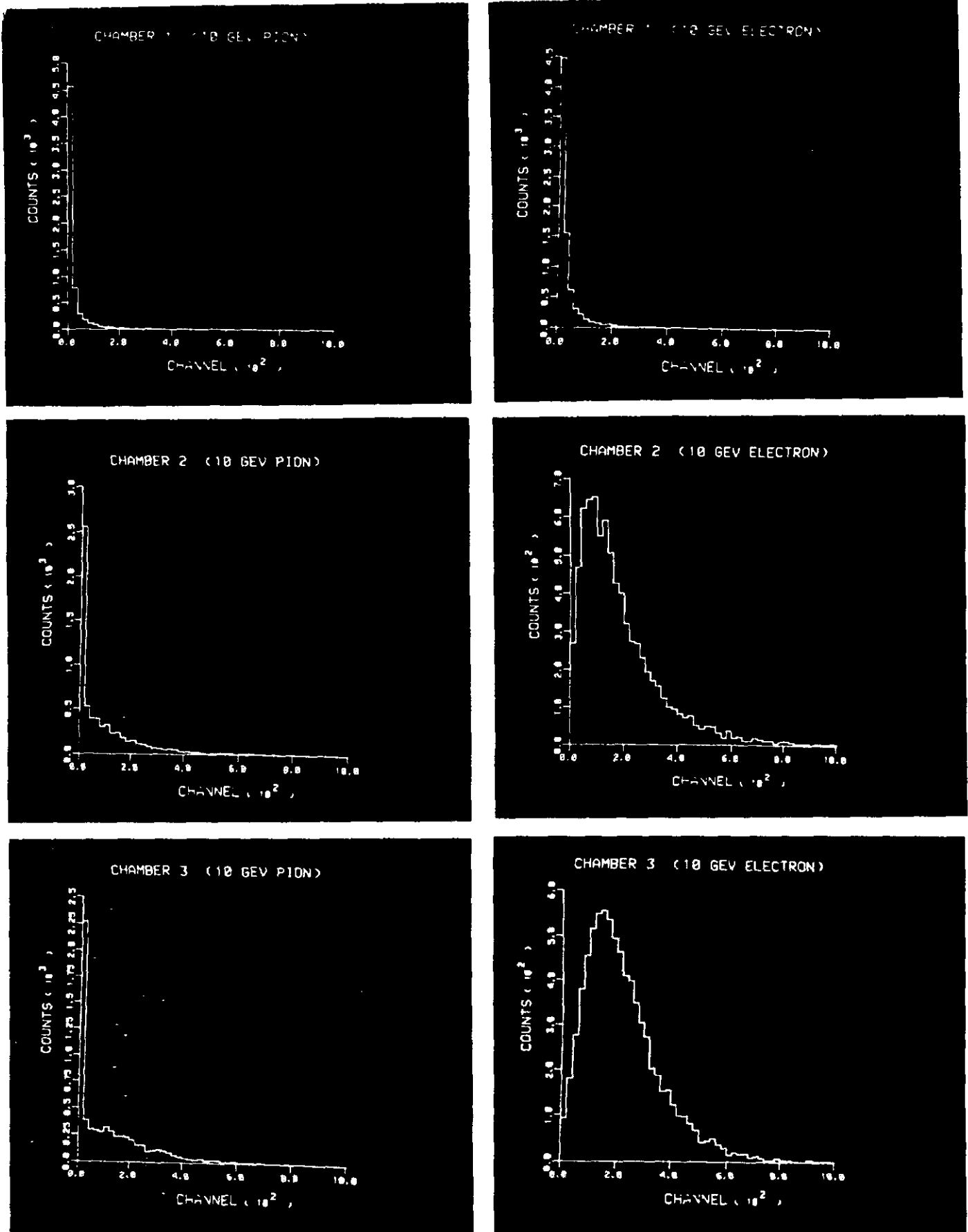


Figure 15 a - Pulse height distribution in chambers 1 through 10 in the Virginia, Maryland, Oxford prototype test detector for 10 GeV incident pions and electrons. There is 1 radiation length of aluminum between each

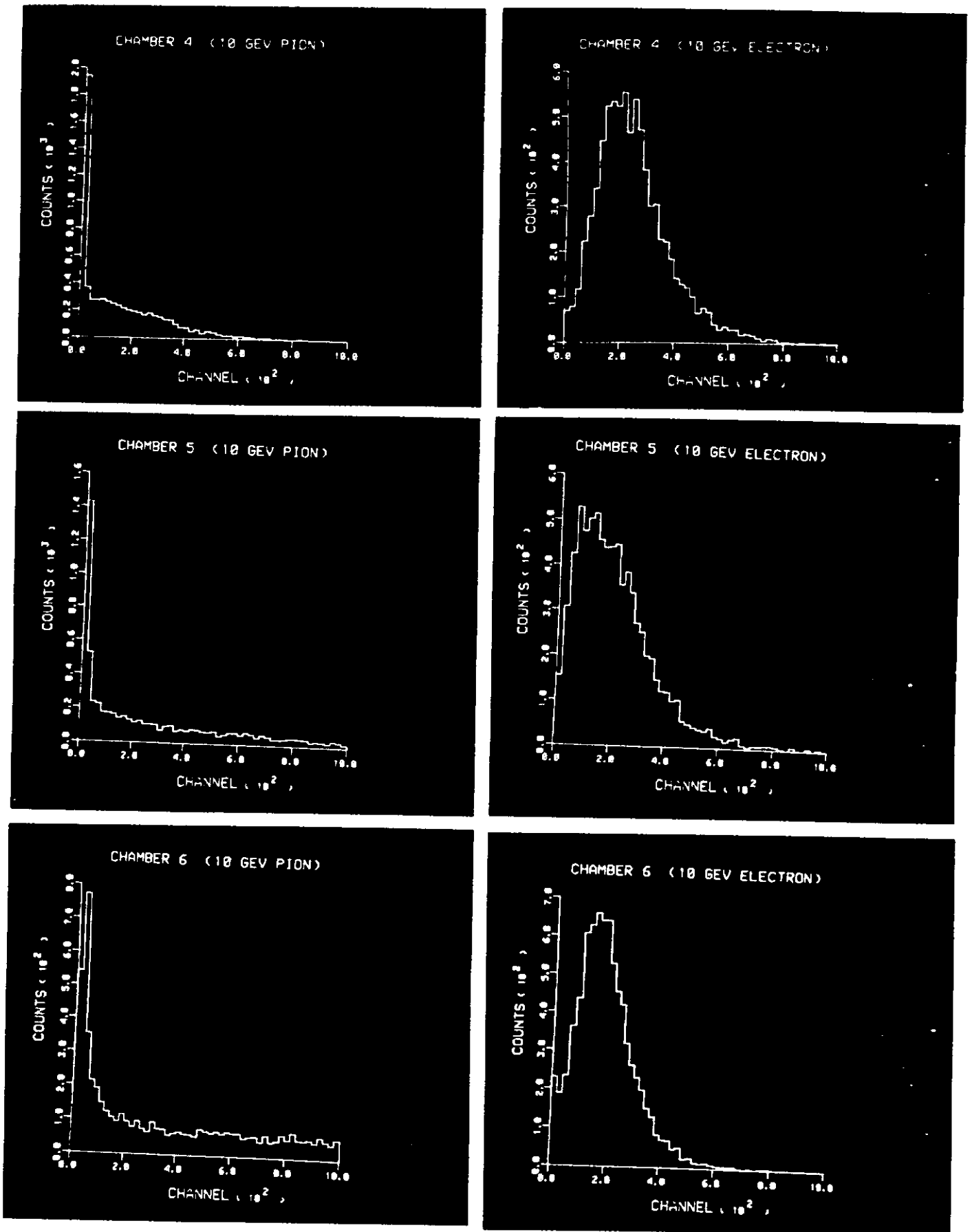


Figure 15b.

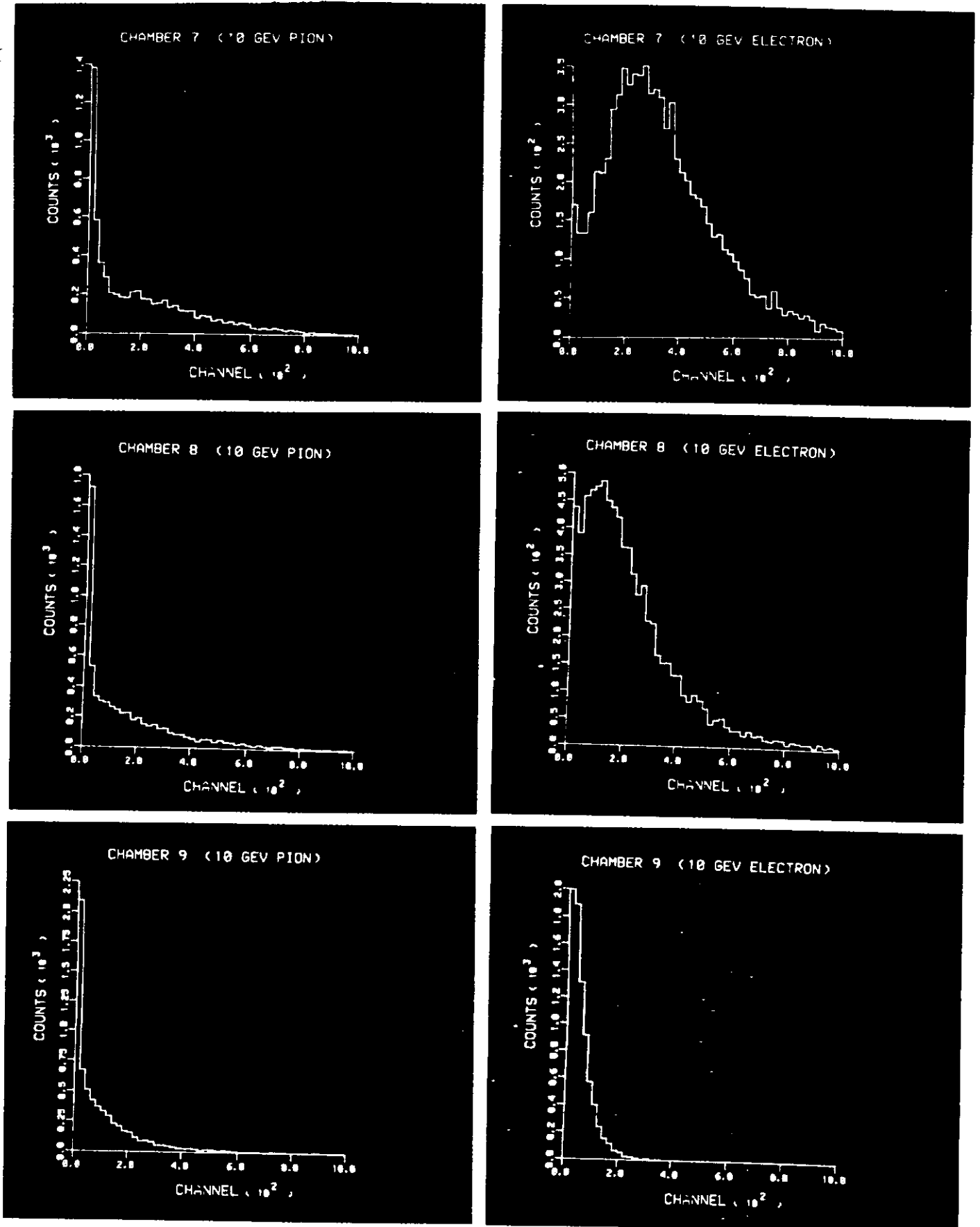


Figure 15c.

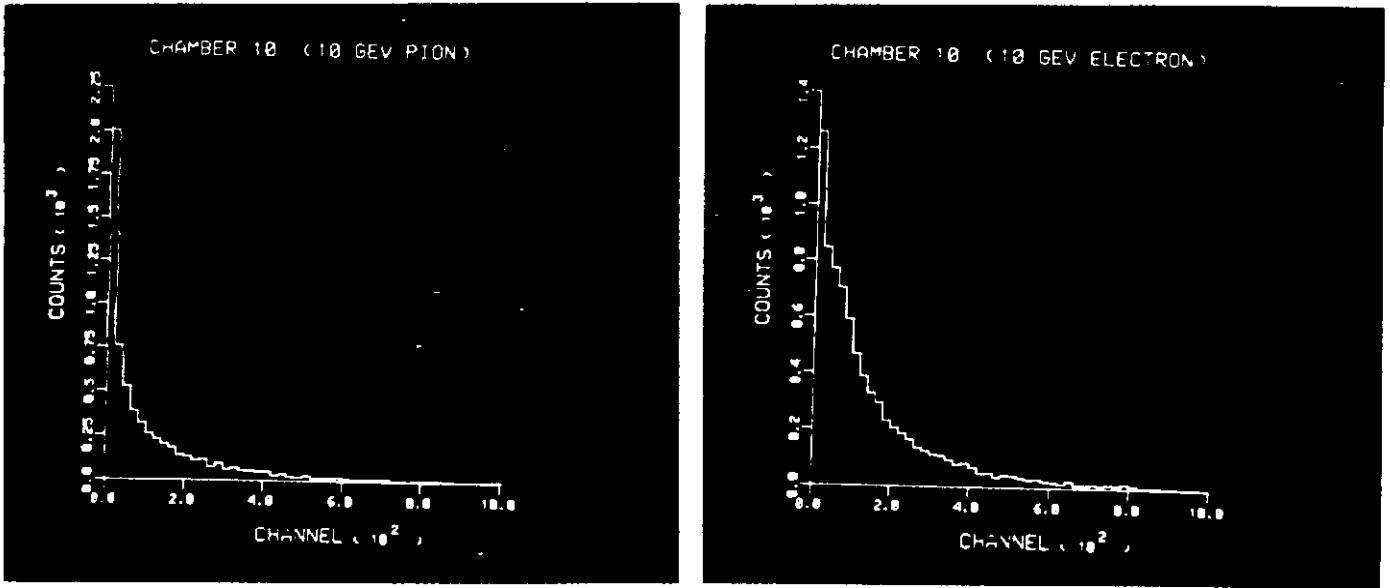


Figure 15d.

be reduced to permit data collection during the routine 400 GeV neutrino beam running. This should begin in June, 1978. A summary of the main properties of the detector are:

Total detector mass:	20 Tons
Electron projected angle resolution:	4mr at 4 GeV
Hadron rejection:	> 300:1
Electron shower sampling step size:	1 length radiation

B. The FIMM collaboration at Fermilab, using the previously described flash chamber detector, also intends to measure the elastic electron scattering reaction.

The test calorimeter was exposed to an electron beam to study the angle resolution of the detector. Figure 16 shows typical electron shower events for 5, 10, 20, 30, and 40 GeV. The transverse and longitudinal development of 10 GeV showers is displayed in Figure 17 where the data from only every ninth plane is displayed for the purpose of clarity. The transverse position of the center of gravity of firing cells was determined for every plane. A straight line was fit to the coordinates of the centers of gravity. The angles of these lines were then plotted and fit to a gaussian distribution. The resulting projected angle resolutions $\sigma(\theta_e)$, were obtained for each electron energy. These resolutions are shown plotted in Figure 18. The data can be described by:

$$\sigma(\theta_e) = (2 + 70/E_e \text{ (GeV)}) \text{ mrad.}$$

For comparison; the measured angle resolution for 10 GeV muons is also shown. It is interesting to compare this angle resolution with those obtained by the Columbia, BNL collaboration⁴ used in the Fermilab 15 ft. Bubble Chamber and in Gargamelle⁵ at CERN. Neutrino electron elastic scattering events have recently been observed in both of these chambers. The angle resolutions obtained in the bubble chambers at the mean observed electron energies are displayed in Figure 18. It can be seen that the angle resolution of the FIMM detector is about a factor of two better than that of Gargamelle and comparable to the 15 ft. chamber result.

It is also interesting to compare the electron energy resolutions in the three detectors. At an energy of 25 to 30 GeV corresponding to the mean electron energy observed in these elastic scattering events, the approximate electron energy resolutions are:

± 10% FIMM
± 30% 15' B.C.
± 50% Gargamelle

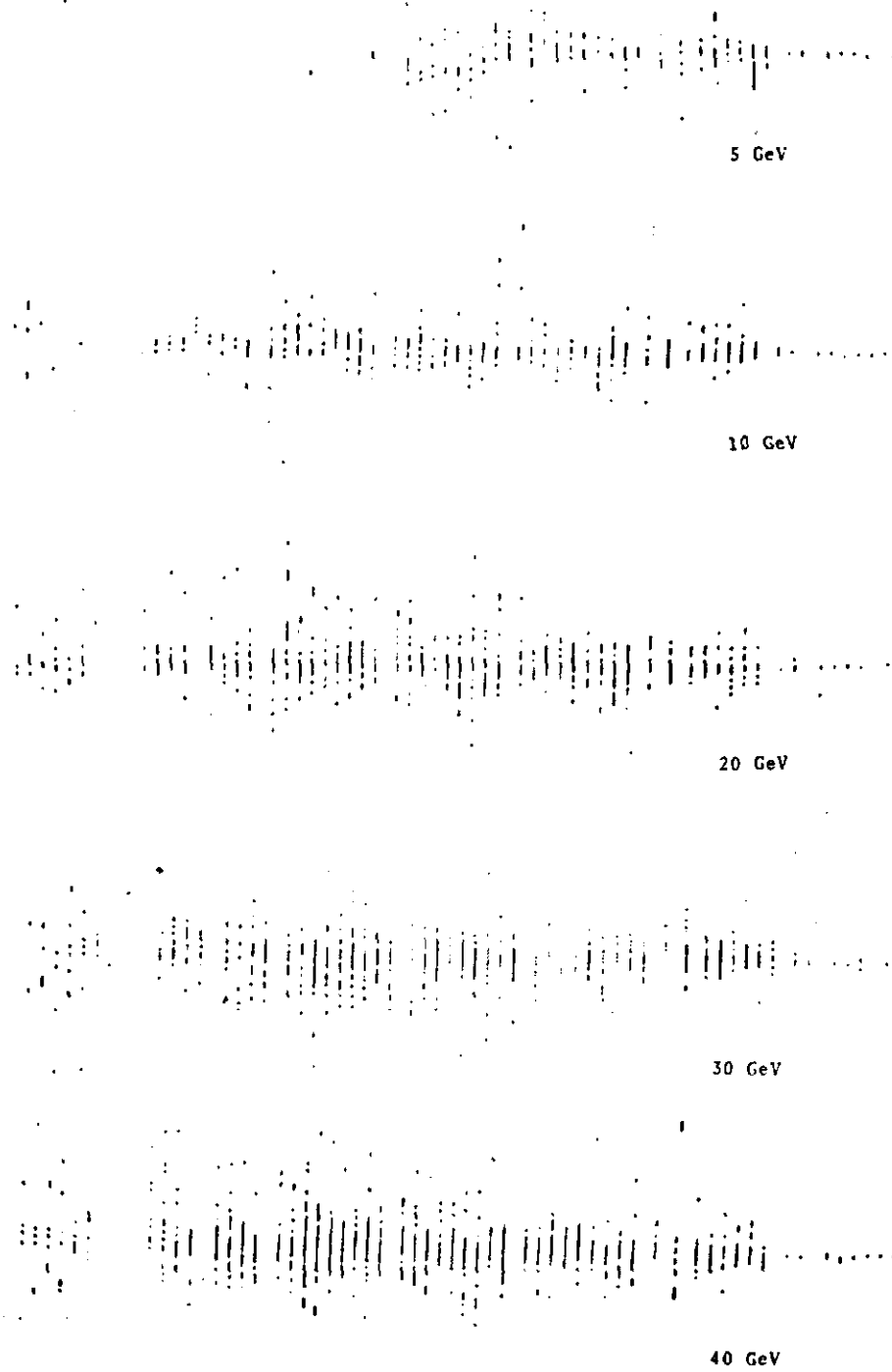


Figure 16. - FIMM test calorimeter photographs of incident electron showers. The energy of the electrons is , indicated in each case.

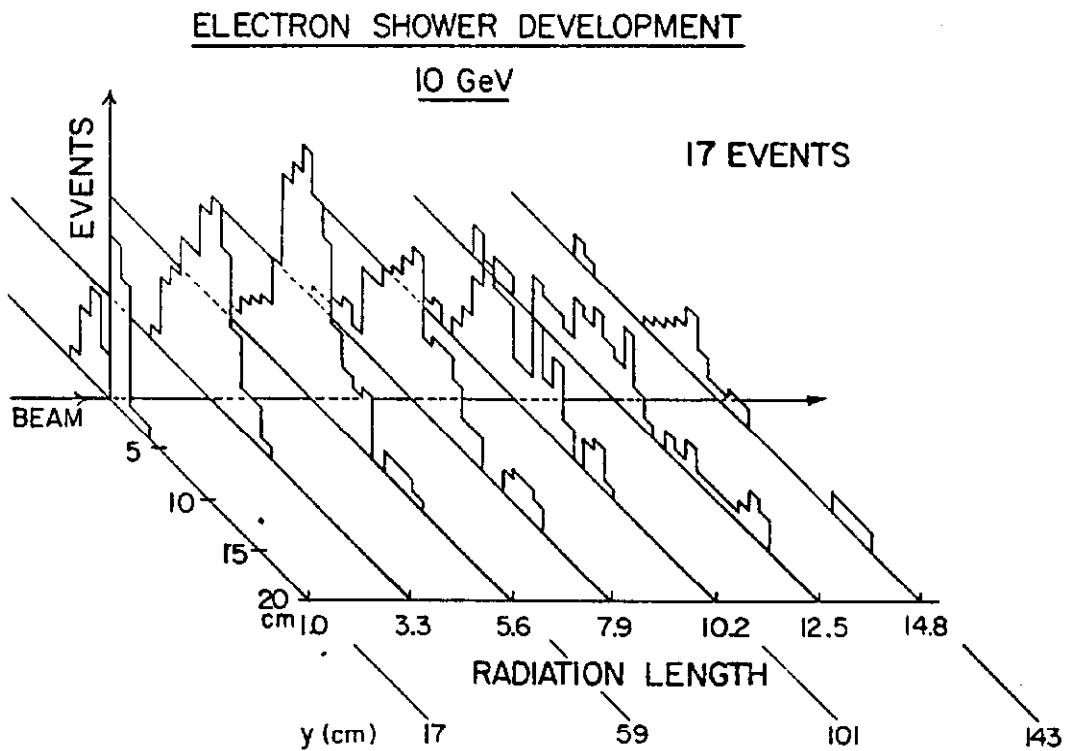


Fig. 17

Figure 17. - Transverse and longitudinal structure of 10 GeV electron showers in the FIMM test calorimeter. Only every ninth plane is shown for clarity.

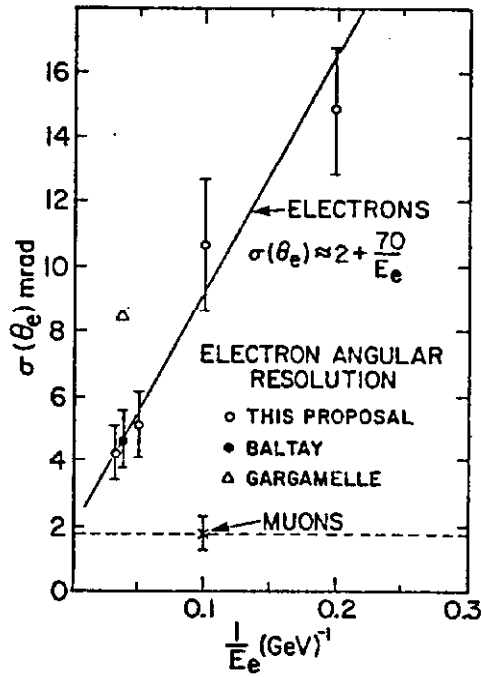


Figure 18. - The projected angle resolution $\sigma(\theta_e)$ for electron shower development is shown plotted against the inverse of the electron energy. The data was obtained with the FIMM test calorimeter. For comparison, the angle resolutions are shown for the Fermilab 15 ft. and Gargamelle Bubble Chambers.

The measured electron energy resolution for the FIMM detector is constant (+ 10%) for the energy range 5 - 40 GeV. Hadron discrimination is achieved by measurement of the transverse and longitudinal structure of the shower. A preliminary lower limit of 100:1 pion rejection has been measured, but it is anticipated to be considerably better when the data has been fully analyzed.

A summary of the main properties of the FIMM detector relevant to this process are given below:

1. Total detector mass: 400 tons
2. Electron projected angle resolution:
 $\sigma(\theta_e) = 2 + 70/E_e(\text{GeV})$ mrad
3. Electron energy resolution: $\sigma(E_e)/E_e = \pm 10\%$
4. Hadron Rejection: > 100:1
5. Electron Shower Sampling Step Size:
9% Radiation Length

C. The CHARM collaboration, whose detector has already been described, also intends to study the neutrino electron elastic scattering reaction. This group has exposed a test calorimeter to a 6.1 GeV/c beam containing both electrons and pions. Using similar methods to that described for the FIMM detector, they obtained an angle resolution for electrons of 15.5 mrad at 6.1 GeV/c. The test data is shown in Figure 19. This group has investigated the pion rejection obtained from cutting on the transverse width of the shower. Figure 20 shows that if a cut is made at 6.2 cm on the r.m.s. width of the shower, then one can obtain electron and pion efficiencies of 95% and 0.5% respectively. The main properties of this detector are:

1. Total detector mass: 200 Tons
2. Electron projected angle resolution:
15.5 mrad at 6.1 GeV/c
3. Hadron rejection: > 200:1
4. Electron shower sampling step size:
1 radiation length.

D. A Brookhaven, Pennsylvania collaboration⁶ have recently indicated their intent to construct a detector at BNL whose principle objective will be a study of neutrino electron elastic scattering. Other semi-leptonic exclusive processes will also be studied.

A schematic of one detector module is shown in Figure 21. This module would be repeated for a total mass of about 150 tons. A unique aspect of this design is that the target material is totally live. The liquid scintillator used for this purpose would be viewed by about 3,000 photomultipliers.

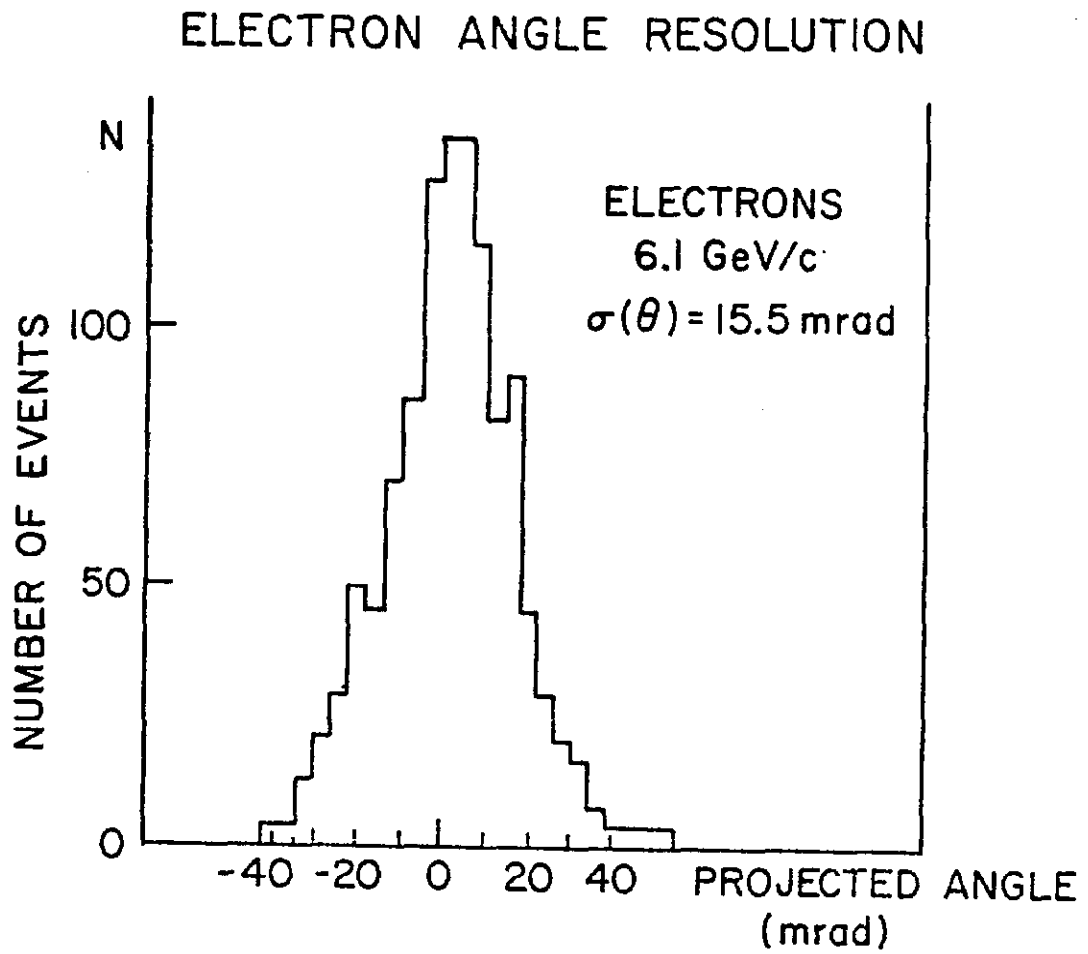


Figure 19. - The distribution of electron events versus projected angle is shown for the CHARM detector.

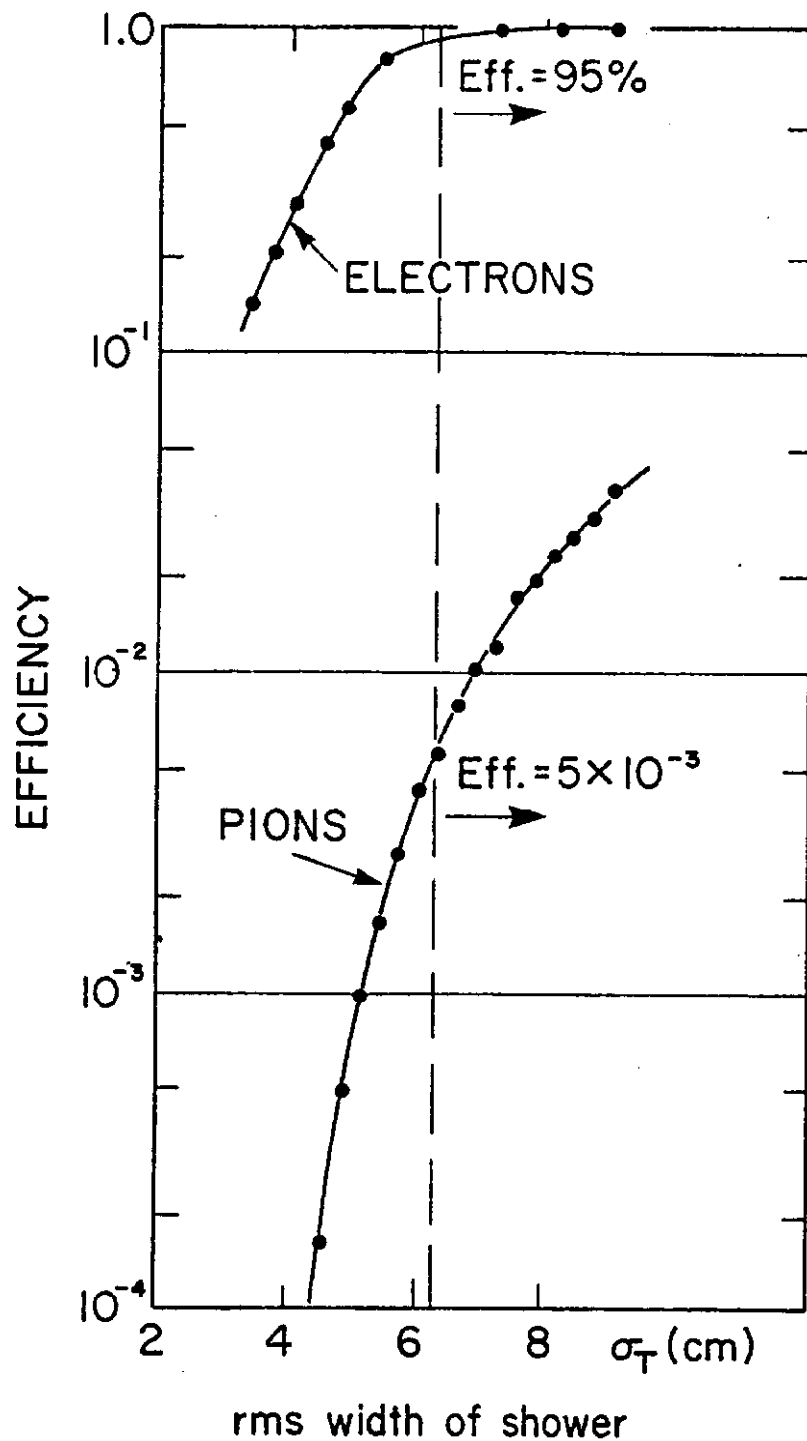


Figure 20. - The efficiency of electron and pion detection is plotted versus the r.m.s. width of the shower. The shower width is obtained by projecting down the full length of the longitudinal development of the shower. The data is for the CHARM detector.

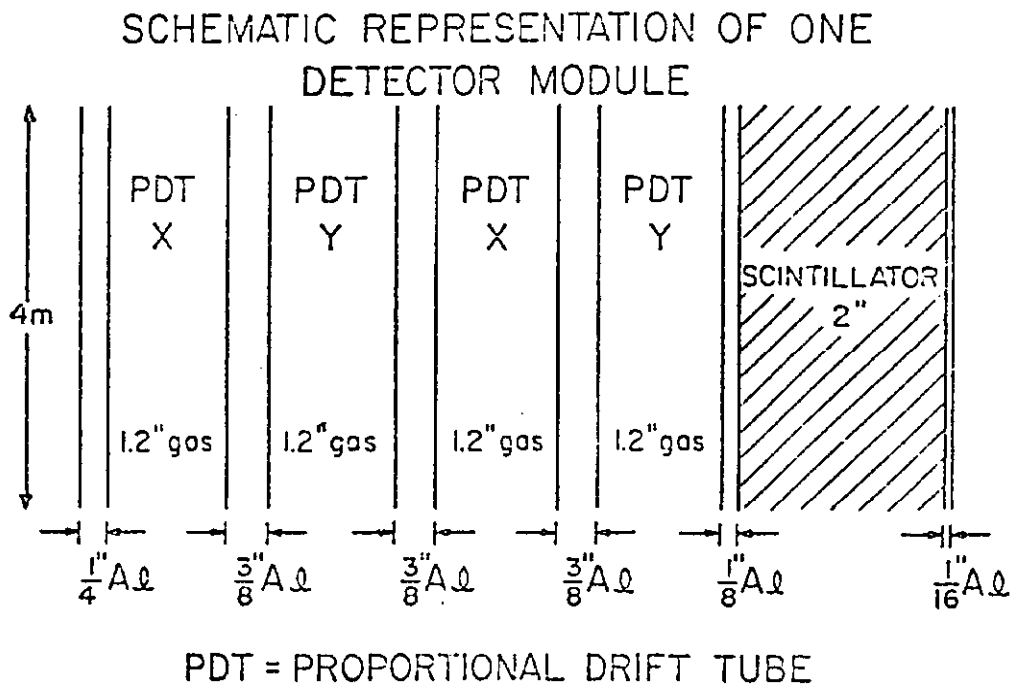


Figure 21. - Schematic drawing of the proposed BNL, Pennsylvania detector for studying neutrino electron elastic scattering.

No estimates or measurements have been made of the angle and energy resolution for electrons.

E. A University of California at Irvine and Los Alamos collaboration is building a detector to study the reaction:



This is the only one of the five experiments discussed, which will permit the study of electron type neutrino scattering. This is due to the intense ν_e beam available from the LAMPF beam dump where π 's are produced, stop and decay, producing μ 's which also stop and decay. The ν_e flux through the detector is $3 \times 10^7 \text{ cm}^{-2} \text{ sec}^{-1}$. The detector is being planned to have a total mass of about 10 tons. It will be a sandwich of flash chambers and thin scintillation planes. The expected event rate is 2 events per day.

3. Search for Short-Lived Particle Production by Neutrinos

In the last two years, there have been several experiments carried out at Fermilab and CERN with the use of large emulsion stacks. These have been placed in both charged particle and neutrino beams in an effort to detect the production of short-lived particles. A further step was taken at CERN, in the use of emulsion as a target, followed by a downstream "multi-particle spectrometer." An emulsion stack was placed at the front of the BEBC chamber and tracks emerging from neutrino interactions in the emulsion were followed, momentum analyzed and, in some cases, identified in the bubble chamber. This data is being analyzed.

Two new experiments at Fermilab are being set up and should begin taking data within the next few months. We discuss these in turn.

A. Experiment E-531 at Fermilab is a collaboration of Fermilab, Kobe University, McGill University, Nagoya University, Ohio State University, Osaka City University, and University of Toronto.

A schematic layout of the detector is shown in Figure 22. Twenty five liters of emulsion are used as the target and shown at the extreme left of the Figure. Tracks emerging from the emulsion traverse a set of drift chambers, DC I, an analysing magnet and a further set of drift chambers, DC II. The spatial resolution of the drift chambers is about 200 microns full width at half maximum. The time of flight of particles is determined by two planes of scintillation counters. The measured time resolution is 80 to 90 pico seconds which permits π , K separation up to

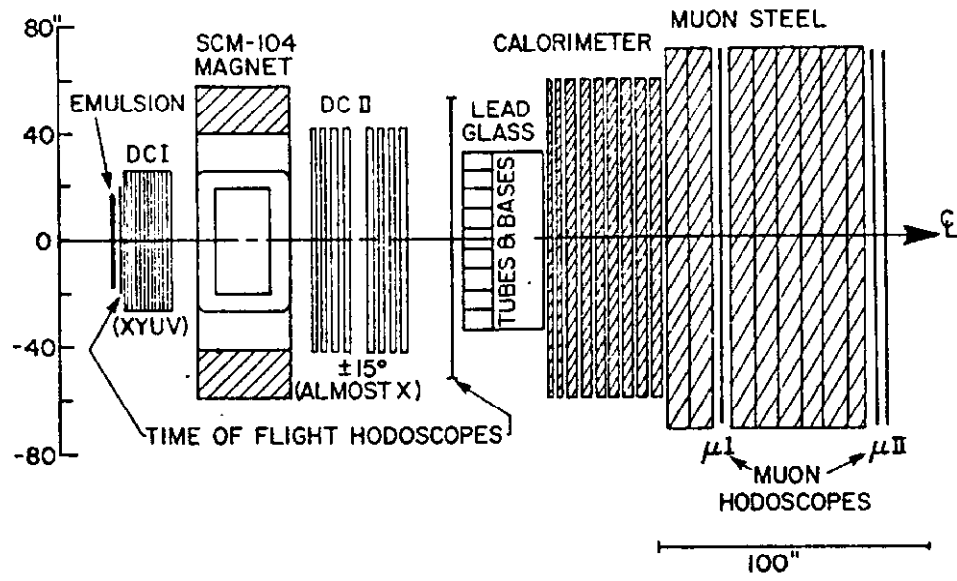


Figure 22. - Schematic drawing of the detector for Experiment E-531 at Fermilab to study short lived particle production by neutrinos.

about 3 GeV. A wall of lead glass Cerenkov counters provides gamma ray and electron detection with a resolution:

$$\sigma(E)/E \approx 0.18/\sqrt{E(\text{GeV})}$$

A hadron calorimeter and muon filter completes the spectrometer.

Preliminary runs are taking place in the summer and the full data collection run will begin in October, 1978. It is planned to use 3×10^{18} protons at 400 GeV and the double horn focussed neutrino beam. A total of 3300 neutrino interactions are anticipated in the emulsion, of which 2,000 may be found at the expected 60% scanning efficiency.

Events in the emulsion target are tagged by the spectrometer and by extrapolation of trajectories the approximate location of the vertex can be determined. Each event will be scanned for decays of short-lived particles in the range 0.005 to 10mm in track length downstream of the vertex. This corresponds to particle lifetimes in the approximate range $3 \times 10^{-15} \lesssim \tau \lesssim 10^{-11}$ seconds.

The expected scanning speed is 1,500 events/year, based on scanning for events initiated by a pion beam. Hence, several hundred events are expected to have been analyzed by the middle of 1979.

B. Experiment E-553 at Fermilab is a collaboration of Cornell, Fermilab, Pittsburg, Lund, Sydney, and York University.

This experiment is similar to the former one but has a unique feature to aid in the finding of events in the emulsion. Fifteen liters of emulsion interspersed with special spark chambers act as the target. A downstream magnetic spectrometer is followed by shower counters and hadron calorimeters constructed with flash chambers. The special spark chambers use glass plates on which an evaporated gold electrode has been deposited. A spark causes gold to be removed from the glass at the precise location of the spark. The resulting spatial resolution of the track is better than 350 microns without the need for precision optics over a large area. Because of the close proximity of the special spark chambers and layers of emulsion, the search volume for events in emulsion is reduced by a factor of about 100 over previous experiments.

The same neutrino beam as for the previous experiment will be used to obtain about 300 neutrino and 40 anti-neutrino initiated events. It is hoped to follow this initial run with further runs during 1979.

4. The Liquid Argon Time Projection Chamber

A California Institute of Technology, University of Irvine, Fermilab collaboration, (P-601), and a group⁷ at Harvard have independently proposed a high resolution liquid argon time projection chamber for the next generation of counter neutrino experiments.

The detector measures the time of arrival and pulse size of the electron image of an event drifting on to an array of sensing electrodes. The time and x, y coordinates are used to reconstruct the image of each track. The pulse size can be used for particle identification. No amplification of the signal occurs in the liquid argon. Spatial resolutions of about 1 millimeter can be expected over drift distances of 0.5 meters.

Crucial to the implementation of these ideas is the behavior of electrons drifting large distances in the liquid. While argon itself should not present any problems, small amounts of impurities, < 50 parts per billion of O₂ could cause significant attenuation of the signal. Both of the proponents of this new technique have studied some of the relevant properties of drifting free electrons in liquid argon. Their⁸ most important result, shown in Figure 23, is that ionization electrons will drift over distances of several cms in an electric field of a few kV-cm⁻¹ with little attenuation. The attenuation length for electrons is probably greater than 50 cms. Longer drift distances are now being studied. It appears reasonable to say, however, that the basic feasibility of the time projection liquid argon chamber has now been established.

Before a large scale detector can be built, it is important to study various additional features. Di-electrics and insulators will be needed to handle the required high voltages. Therefore, the pollution properties of various materials will have to be studied to establish acceptable construction methods. In addition, the basic questions of longitudinal and transverse diffusion of electrons as a function of drift distance should be studied.

The problem of obtaining maximum information for particle track reconstruction from the small amounts of ionization in the liquid has been discussed recently in a paper by Gatti, Padovini, Quartapelle, Greenlaw, and Radeka⁹. They describe the basic concepts of optimum electrode geometry and signal processing for time projection ionization chambers. The signals induced by particle tracks on the sensing electrodes are calculated by

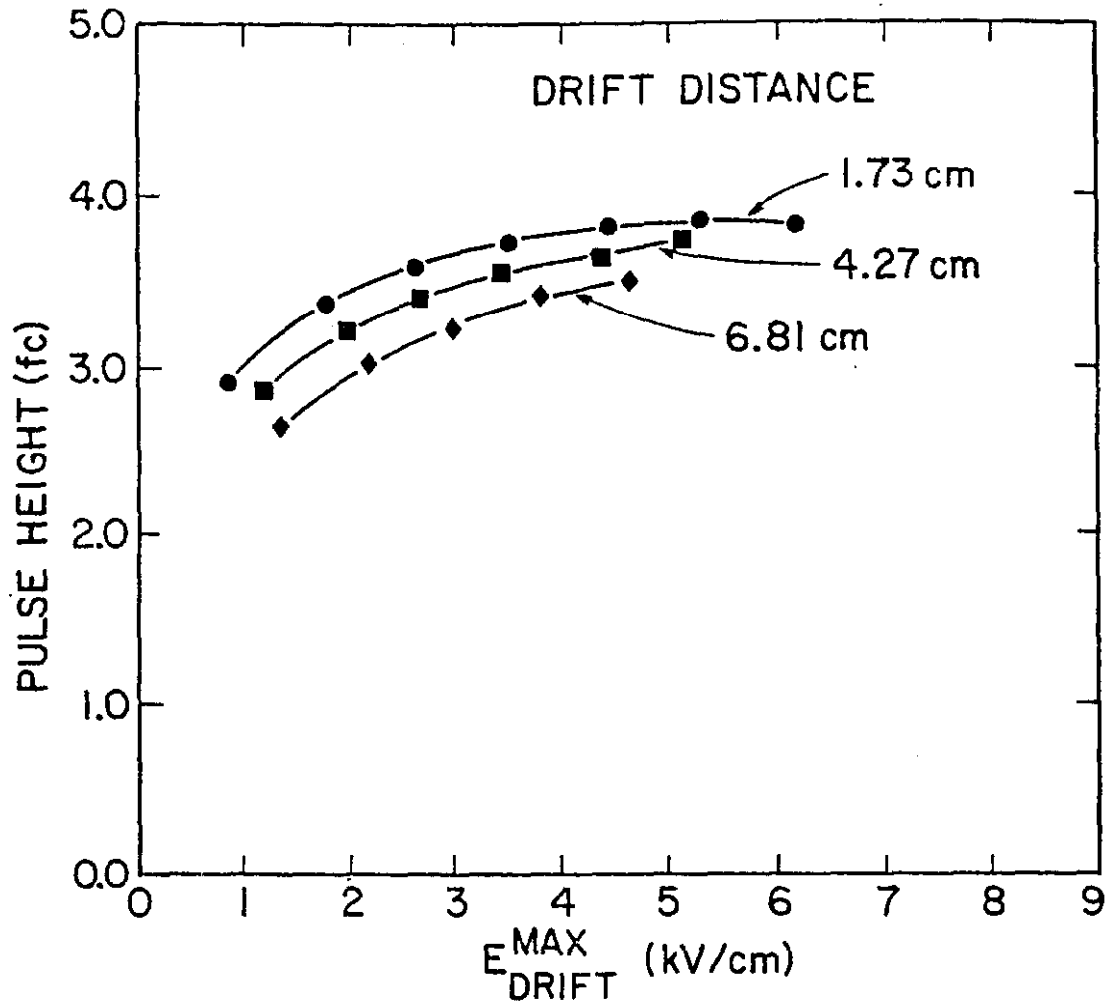


Figure 23. - The pulse height for the internal conversion peak using ^{137}Cs is shown versus E_{drift}^{max} . Data from three drift distances are shown. The decrease in the collected charge with distance at fixed E_{drift}^{max} indicates that the electron drift distance, λ_D is at least 35(50)cm with E_{drift}^{max} at 2(4) kV-cm⁻¹.

means of a detailed study of possible electric field configurations. Suitable signal processing filters are designed in order to achieve nearly equal position resolution in the three-space coordinates. The electronic noise limits the position resolution of a single track to a few tenths of a millimeter and the capability to resolve and measure closely spaced multiple tracks to a few millimeters.

It is clear that the time projection liquid argon chamber is a concept which will receive much more attention in the coming years. At Fermilab a 5 to 10 ton prototype calorimeter is being designed and will be constructed in the next year.

5. The Liquid Argon Iron Plate Calorimeter

A Harvard, University of Chicago and University of Illinois collaboration (P-541) has proposed construction of a new neutrino detector at Fermilab. The detector consists of four modules, each made up of a calorimeter, drift chambers, scintillation counters, and a 10 kilogauss superconducting magnet for muon momentum analysis. The calorimeter is based on a novel liquid argon iron plate design which will be described in more detail.

The liquid argon container is 2.5m x 2.6m x 5m giving a fiducial mass of 73 tons within a 2m x 2m x 4m fiducial region. Iron plates, each 3mm thick, are spaced 4mm apart throughout the liquid argon volume as shown in Figure 24. Alternate iron plates are segmented in 2cm wide strips with strips alternating in the x and y directions. Five consecutive x strips and 5 consecutive y strips are ganged together to give coordinate measurements every 0.75 interaction length. This gives an average of 10 x, y points per shower which are expected to be adequate for a good measurement of its direction.

A prototype module of this detector was constructed with adequate size to contain the hadronic shower. Preliminary data has recently been obtained in a low energy test beam at Fermilab. The linear response of the detector versus hadron energy is shown in Figure 25. At this stage, the data on resolutions has been analyzed in a very preliminary fashion and it is expected that the results given are upper limits to the true resolution. A plot of $\sigma(E_H)/E_H$ is shown versus E_H in Figure 26.

The resolution is roughly consistent with $75\%/\sqrt{E_H}$. Some earlier data obtained with an iron, liquid argon calorimeter at CERN is shown for comparison.

The angle resolution of the hadronic cascade has been obtained using algorithms like those described earlier in this report. Once again, it is expected that these results will be improved with further analysis. The result of the initial analysis is

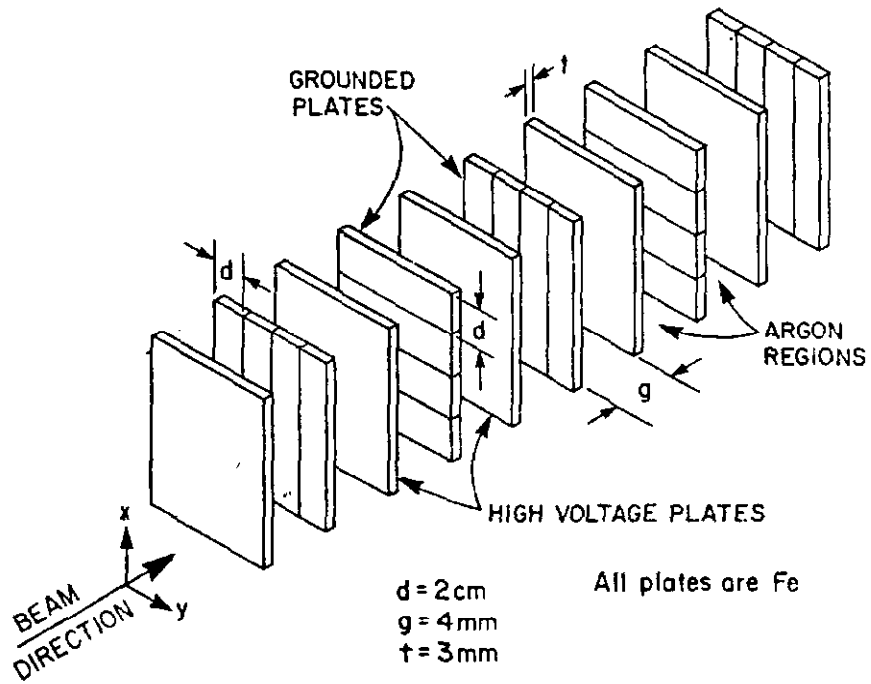


Figure 24. - Iron plate structure of the liquid argon iron plate calorimeter.

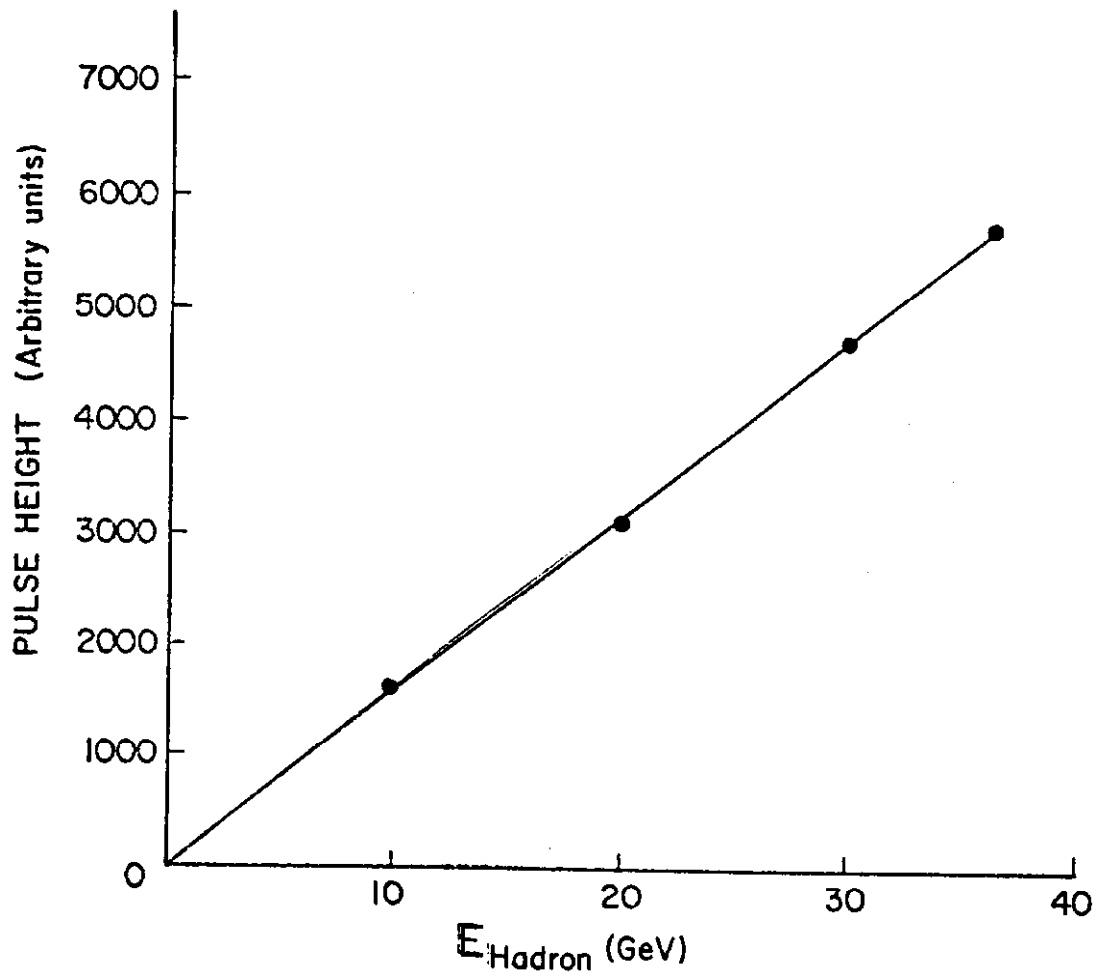


Figure 25. - Pulse height summed over all plates versus hadron, energy for the liquid argon iron plate calorimeter. The response is seen to be linear.

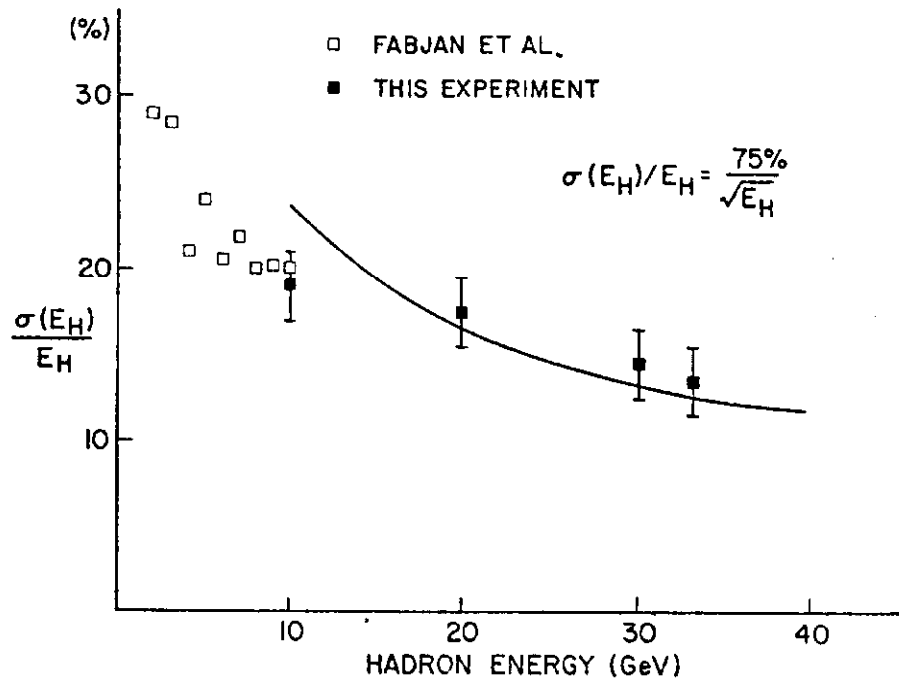


Figure 26. - Energy resolution of the liquid argon iron plate calorimeter. Some early data from CERN is shown for comparison.

shown in Figure 27. The angle resolution is consistent with an expression of the form:

$$\sigma(\theta_H) = (15 + 433/E_H) \text{ mrad}$$

This is an interesting new technique which will be pursued by additional analysis and, hopefully, more data at higher energies.

6. The Liquid Argon Bubble Chamber with Electronic Readout

A group¹⁰ at Fermilab has proposed an optical detector that combines the visual imagery of a bubble chamber with the fine grain calorimetry and muon identification of counter experiments. It consists of ten in-line modules, each containing a large cylindrical liquid argon bubble chamber and magnetized iron spectrometer. There are several technological innovations: Liquid argon as a bubble chamber fluid; electronic recording of bubble images on videotape; ionization drift in the liquid argon over one meter distance; a new approach to expansion bellows and cryostat design.

Each module of the detector functions largely independently. One module is shown in Figure 28. The liquid argon bubble chamber has an enclosed volume of 10m x 2.5m diameter. Ionization electrons are drifted to a collection tube on the axis of the chamber. There they are collected in 17cm longitudinal segments (one radiation length) amplified, and the charge is recorded as a function of drift time (hence radius). An iron-argon calorimeter following the bubble chamber assures complete containment of all showers occurring within the fiducial region.

This is an imaginative approach, requiring the most advanced technology on several fronts at the one time. The proponents are, therefore, requesting support during the coming year to carry out prototype tests on some aspects of the design.

7. The Water Cerenkov Neutrino Detector

A proposal has been made to Fermilab by physicists¹¹ at the University of Chicago to construct a massive new neutrino detector to study the neutrino electron elastic scattering reaction.

The detector is a tank containing distilled water. It is 4 x 4 x 60 meters and is viewed by 2,000 photomultipliers. The neutrino electron scatters are characterized by the appearance of an isolated electron at very small angles to the beam. The Cerenkov radiation of the electron shower conveys the angular information of the electron shower to the walls of the detector. The detectors at the walls of the tank have a response which is sensitive to the angle of a single collimated source of radiation.

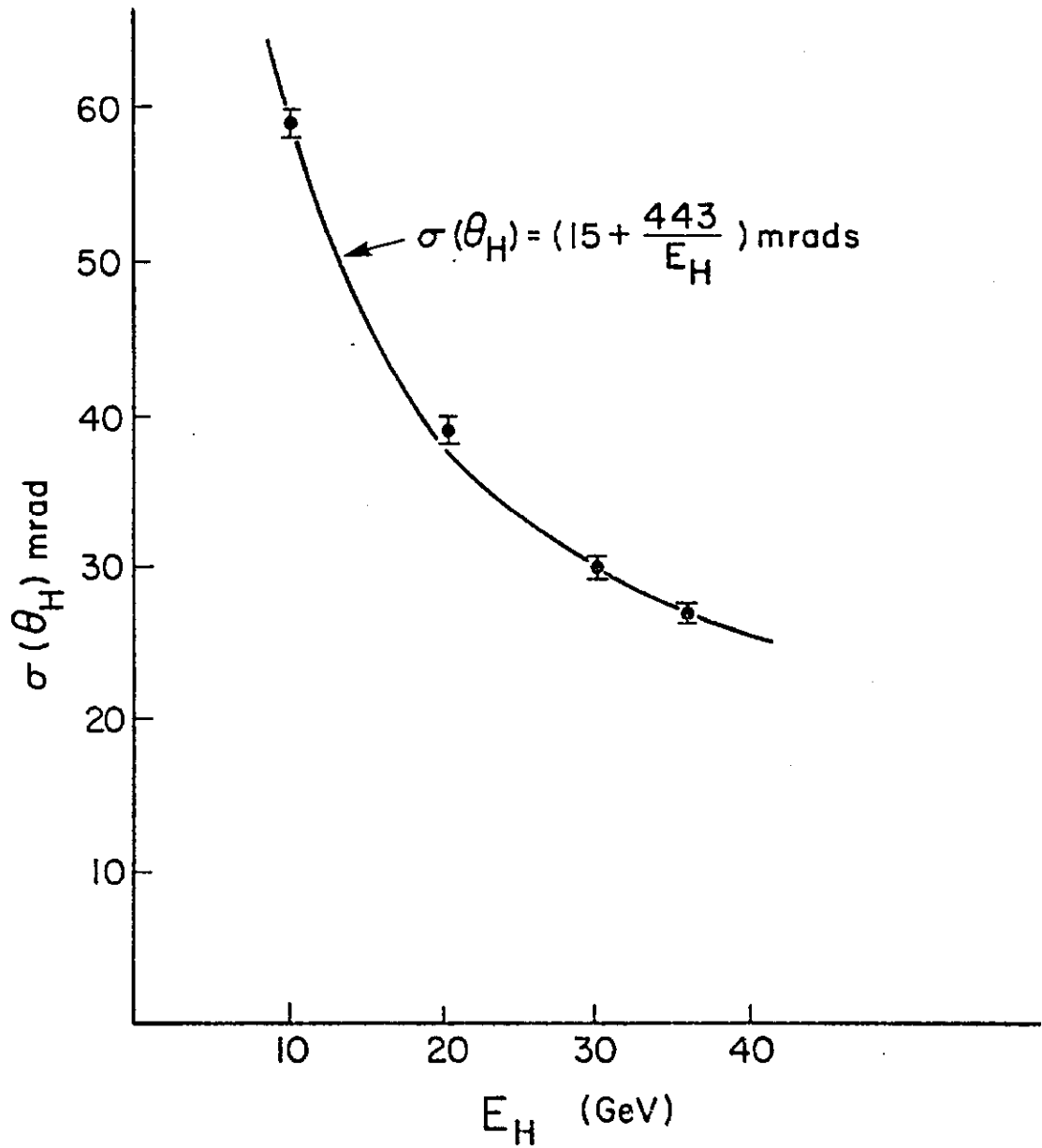


Figure 27. - Projected angle resolution for hadron cascade development is shown plotted versus hadron energy. The data is from the liquid argon iron plate calorimeter.

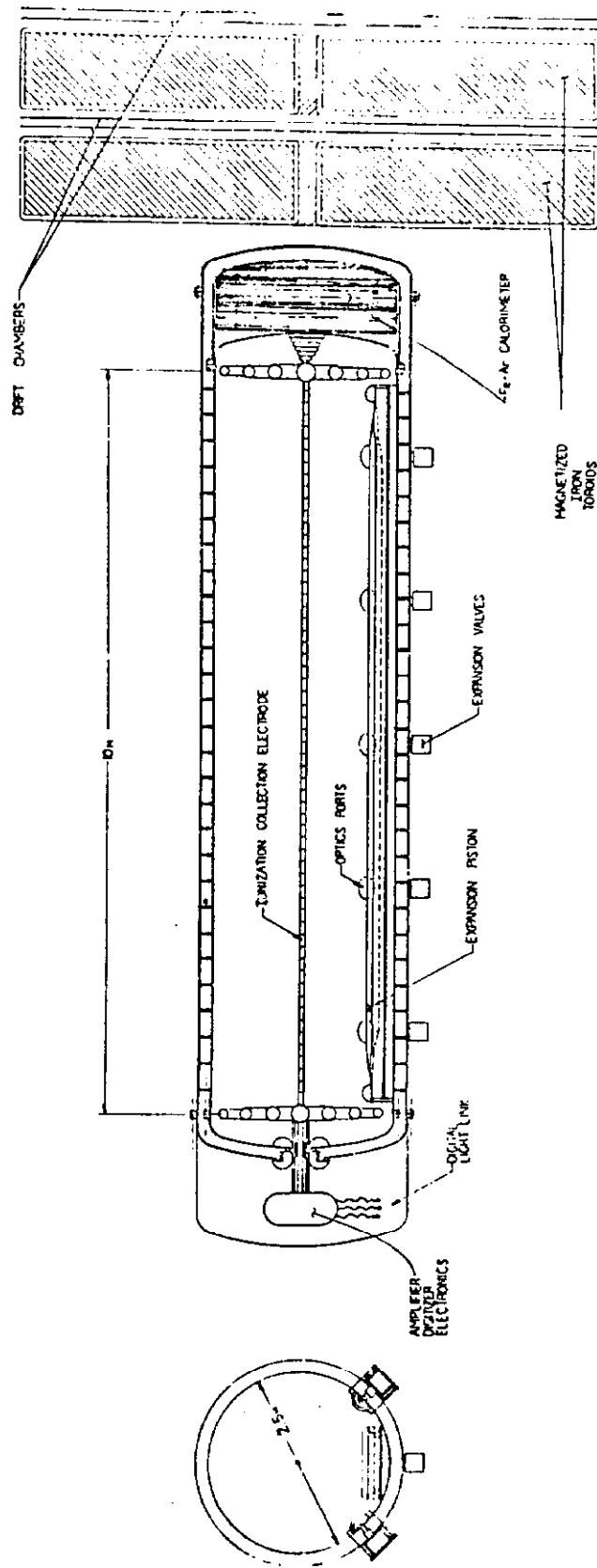


Figure 28. - Cross section of one detector module of the liquid argon bubble chamber with electronic readout.

The principle of the detector is illustrated in Figure 29a, in which a muon is shown traversing the detector. The Cerenkov light is viewed by two windows parallel to the radiation. If the muon trajectory is exactly parallel to the windows, then the Cerenkov light for a fully relativistic particle will be exactly totally internally reflected at the window-air interface, and no light will emerge. If the muon is directed towards one window as in Figure 29b, light will emerge from the window towards which the particle is directed. The directional information can be improved if the windows are tilted with respect to the axis of the detector as shown in Figure 29c. Then, even a parallel track will produce light through both windows. If the windows are tilted at an angle of 25 mrad, one would expect a response as shown in Figure 29d. This provides a quantitative measure of the projected angle of the track of the particle in the range of ± 25 mrad.

A detector design has been studied by computer simulation. An isometric drawing of the proposed detector is shown in Figure 30. There are 2,000 windows with associated photomultipliers. Each window is 35cm wide and 100cm long. The rows are spaced 120cm apart so fifty rows give a detector of 60 meters length. The fiducial volume is considered to be 3m x 3m x 55m giving 500 tons. The range of projected angle over which a quantitative measure of the shower angle can be obtained is ± 75 mrad. The expected angle and energy resolutions for electron showers are shown below:

<u>Electron Energy GeV</u>	<u>$\sigma(\theta)$ Projected (Mrad)</u>	<u>$\sigma(E)/E$ %</u>
5	7.0	5.7
15	5.0	4.6
25	4.0	3.2
35	3.5	3.0

Rejection of backgrounds is the main problem for any detector of neutrino electron elastic scattering. A preliminary Monte Carlo study of hadron rejection has been made and indicates that appropriate cuts can reject neutrino initiated hadron events by a factor of roughly 10^4 , however, there are some uncertainties in this analysis. A more detailed study of this problem is underway. The group plans to construct a prototype module of the detector and test its properties in a beam of pions and electrons.

8. A Search Method of Massive Neutral Leptons

R. Shrock¹², Princeton, has proposed a method to search for the

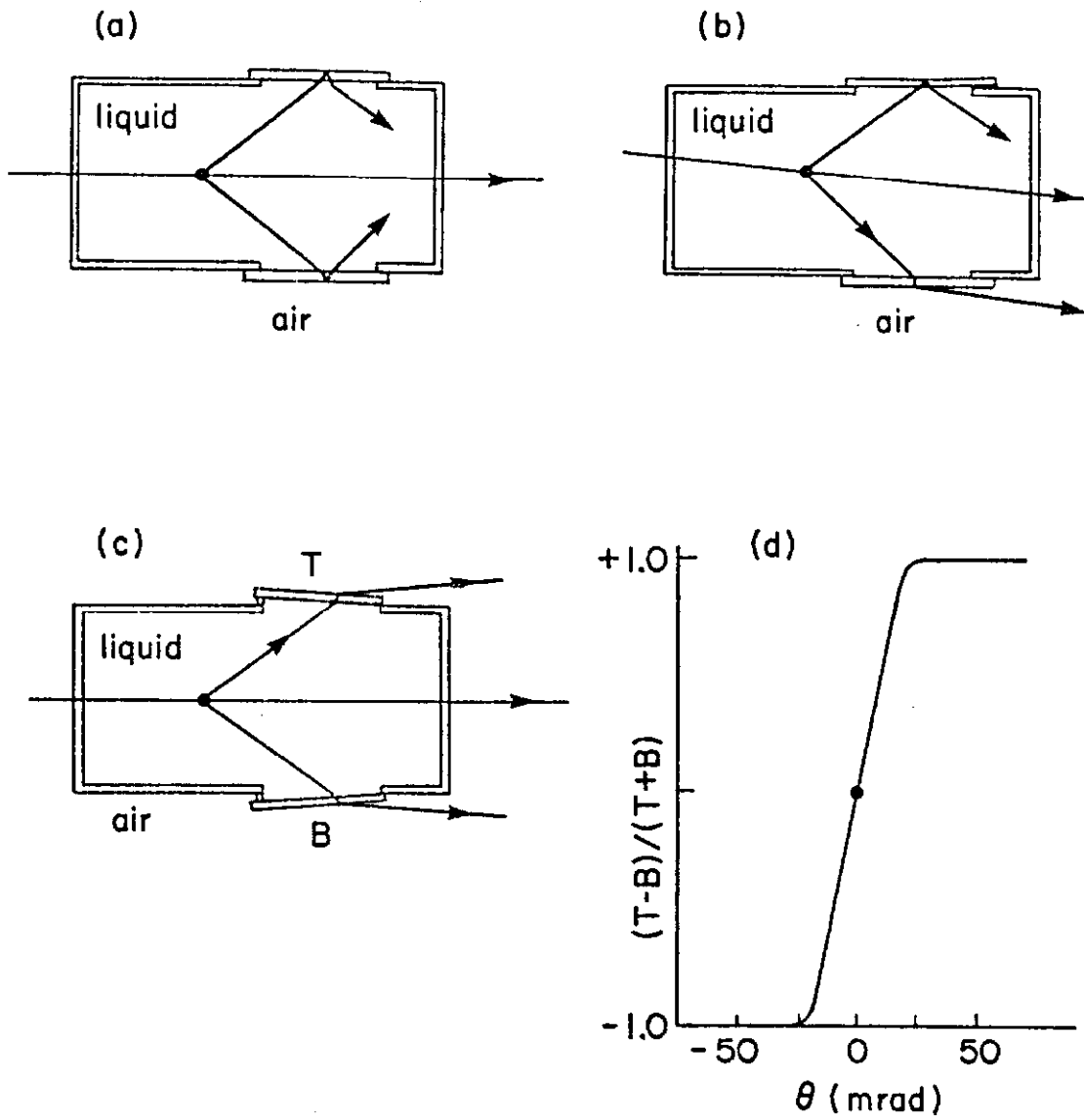


Figure 29. - The concept of the water Cerenkov neutrino detector is illustrated (see the text for details).

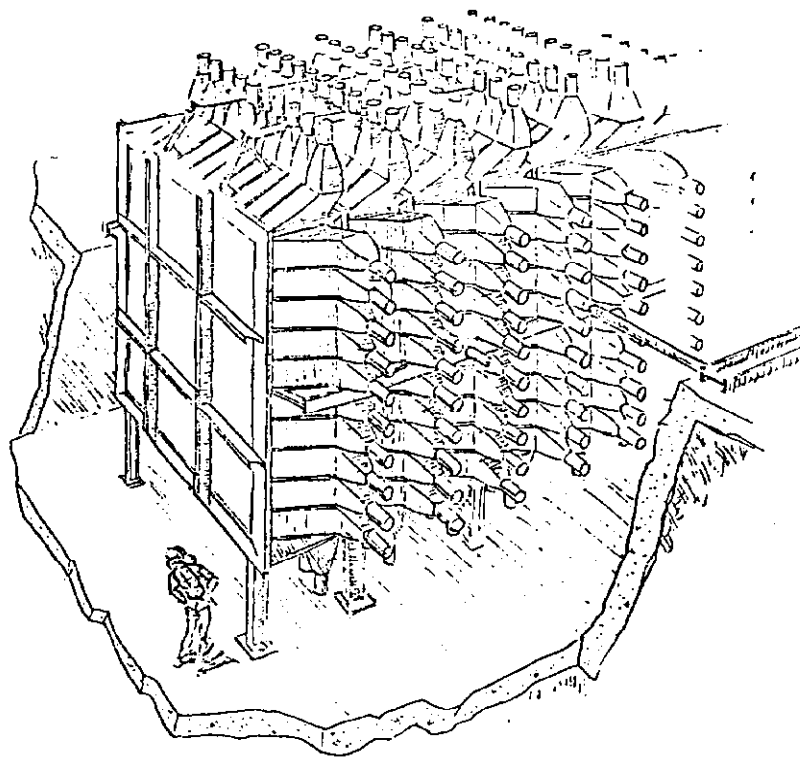


Figure 30. - An isometric view of the water Cherenkov neutrino detector.

existence of stable or unusually long-lived neutral heavy leptons.

It consists of a beam dump, as used recently at CERN for the production of prompt neutrinos, followed by a massive electronic target calorimeter. The crucial aspect of the experiment is the use of timing to an accuracy of approximately 1 nanosecond in order to discriminate between the arrival of massless and massive neutral leptons and to select the latter. Previous experiments have not had the ability to perform this timing of the event relative to the radio frequency structure of the primary proton beam. At Fermilab and CERN there is about 20 and 5 nanoseconds respectively between proton bunches. The longer time interval between bunches available at Fermilab facilitates the measurements. This R.F. structure is preserved by neutrinos from the beam dump, given the existing upper bounds on their masses and the fact that the path length $l \lesssim 1$ km. A timing signal from the R.F. system can be used to determine the time at which the neutrinos will arrive at a particular point in the detector. If these points were the same for a massless and massive lepton, then the latter would lag behind the former by $\Delta t = (l/c) (\beta^{-1} - 1)$. These leptons will in general interact at different points, but this can be taken into account in measuring the relative flight times. The two main sources of error in the time measurement relative to the true time are (1) the finite width of the proton bunches and (2) the measurement error of the longitudinal point of interaction in the detector. Let us suppose that together they produce a total error of about 1.5n sec. This in turn determines the maximum value of β which can be distinguished from unity; it is given by $(\beta^{-1} - 1) = \epsilon$ where $\epsilon = 0.5 \times 10^{-3} (l/1\text{km})^{-1}$. This corresponds to a minimum value of $\gamma^{-1} = M_E/E$ (where $E(M_E)$ is the E° energy (mass) which can be distinguished from zero:

$$\gamma_{(-)}^{-1} = \sqrt{2 \epsilon (1 + \epsilon/2) / (1 + \epsilon)}$$

In some of the E° - induced reactions, it is possible to determine E with an accuracy comparable to that in a regular neutrino experiment. Together with the measurement of γ from Δt , this enables one to compute the E° mass. Taking $E \approx 20$ GeV as a rough value below which the E° flux would be significantly reduced, it is possible to discover an E° of mass $M_E \gtrsim 0.6$ GeV.

It is unlikely that any of the existing neutrino detectors have the capability of performing timing measurements to about one nanosecond. However, it appears feasible to install special counters to provide the required information.

The observation of a delayed lepton signal would represent a major new discovery in weak interactions.

ACKNOWLEDGEMENTS

I would like to thank the many experimenters for providing much of the information in this report. In particular, I acknowledge many stimulating discussions with Professor F.E. Taylor on all aspects of neutrino detector development.

REFERENCES

1. This experiment is described in CERN/SPSC/75 - 59/ P59.
2. M. Conversi, et al., CERN E.P. Internal Report (76-20); F.E. Taylor, et al., I.E.E.E. Transactions on Nuclear Science, Vol. NS-25, No. 1, P312, February 1978.
3. F.J. Sciulli, Calorimeter Workshop, Fermilab, P79, (1975).
4. C. Baltay, private communication.
5. P. Alibrant, et al., Observation and Study of the $\nu_{\mu}e^{-} \rightarrow \nu_{e}e^{-}$ Reaction in Gargamelle at High Energy, Preprint, April 7, 1978, (submitted to Physics Letters B).
6. Letter of Intent from H. White to R. Rau, April 28, 1978.
7. W. Huffman, J. LoSecco, and C. Rubbia, Harvard Preprint, HUHEPL 78-426A.
8. This result was obtained by H. Chen and J. Lathrop, Preprint, UCI-10P19-120, October, 1977.
9. E. Gatti, et al., BNL Preprint, May, 1978.
10. G. Harigel, H. Kautzky, P. McIntyre, and A. VanGinneken, Fermilab Proposal No. 601, May 5, 1978.
11. J.W. Cronin and M.L. Swartz, Fermilab Proposal No. 600, May, 1978.
12. R.E. Shrock, Phys. Rev. Lett. 40, 1688, (1978).